

REPORT DOCUMENTATION PAGE			Form Approved OMB No. 0704-0188	
<small>1. AGENCY USE ONLY (Leave blank)</small> <small>2. REPORT DATE</small> <small>3. REPORT TYPE AND DATES COVERED</small> <small>4. TITLE AND SUBTITLE</small> <small>5. FUNDING NUMBERS</small> <small>6. AUTHOR(S)</small> <small>7. PERFORMING ORGANIZATION NAME(S) AND ADDRESS(ES)</small> <small>8. PERFORMING ORGANIZATION REPORT NUMBER</small> <small>9. SPONSORING, MONITORING AGENCY NAME(S) AND ADDRESS(ES)</small> <small>10. SPONSORING, MONITORING AGENCY REPORT NUMBER</small> <small>11. SUPPLEMENTARY NOTES</small> <small>12a. DISTRIBUTION / AVAILABILITY STATEMENT</small> <small>12b. DISTRIBUTION CODE</small> <small>13. ABSTRACT (Maximum 200 words)</small> <small>14. SUBJECT TERMS</small> <small>15. NUMBER OF PAGES</small> <small>16. PRICE CODE</small> <small>17. SECURITY CLASSIFICATION OF REPORT</small> <small>18. SECURITY CLASSIFICATION OF THIS PAGE</small> <small>19. SECURITY CLASSIFICATION OF ABSTRACT</small> <small>20. LIMITATION OF ABSTRACT</small>				
1. AGENCY USE ONLY (Leave blank)		2. REPORT DATE February 26, 1997		3. REPORT TYPE AND DATES COVERED Technical
4. TITLE AND SUBTITLE Radiation Curing of Fabric Reinforced Elastomeric Composites			5. FUNDING NUMBERS  DAAH04-95-2-0004	
6. AUTHOR(S) Walter J. Chappas Feng-Jon Chang Joseph Silverman			8. PERFORMING ORGANIZATION REPORT NUMBER  MD 950220-7297-36021	
7. PERFORMING ORGANIZATION NAME(S) AND ADDRESS(ES) University of Maryland College Park, MD 20742			10. SPONSORING, MONITORING AGENCY REPORT NUMBER  ARO 34819.1-MS	
9. SPONSORING, MONITORING AGENCY NAME(S) AND ADDRESS(ES) U.S. Army Research Office P. O. Box 12211 Research Triangle Park, NC 27709-2211			11. SUPPLEMENTARY NOTES The views, opinions and/or findings contained in this report are those of the author(s) and should not be construed as an official Department of the Army position, policy, or decision, unless so designated by other documentation.	
12a. DISTRIBUTION / AVAILABILITY STATEMENT  Approved for public release; distribution unlimited.			12b. DISTRIBUTION CODE	
13. ABSTRACT (Maximum 200 words)  Ionizing radiation from cobalt-60 gamma and electron beam sources are used to investigate methods to improve the abrasion resistance of polyurethane elastomers. Radiation curing of acrylated urethane oligomers and grafting acrylonitrile onto polyurethanes were studied. Low energy electron beam and plasma surface treatment was also performed. A special device was developed to measure edge abrasion, i.e. the abrasion of folded surface.  This work demonstrated that radiation grafting techniques are an effective technique for improving the edge abrasion resistance of polyurethane, with minimal changes in the bulk mechanical properties. Best properties were observed in 10% AN/n-hexane solution irradiated to a 10 kGy absorbed dose.				
14. SUBJECT TERMS Polyurethane Elastomers Abrasion Radiation			15. NUMBER OF PAGES 110	
17. SECURITY CLASSIFICATION OF REPORT UNCLASSIFIED			16. PRICE CODE	
18. SECURITY CLASSIFICATION OF THIS PAGE UNCLASSIFIED			19. SECURITY CLASSIFICATION OF ABSTRACT UNCLASSIFIED	
			20. LIMITATION OF ABSTRACT UL	

RADIATION CURING OF FABRIC REINFORCED ELASTOMERIC COMPOSITES

FINAL REPORT

WALTER J. CHAPPAS  
FENG-JON CHANG  
JOSEPH SILVERMAN

JANUARY 27, 1997

U.S. ARMY RESEARCH OFFICE

DEPARTMENT OF MATERIALS & NUCLEAR ENGINEERING  
UNIVERSITY OF MARYLAND  
COLLEGE PARK, MD 20742-2115

APPROVED FOR PUBLIC RELEASE  
DISTRIBUTION UNLIMITED

19970521 138

THE VIEWS, OPTIONS, AND/OR FINDINGS CONTAINED IN THIS REPORT ARE  
THOSE OF THE AUTHORS(S) AND SHOULD NOT BE CONSTRUDED AS AN OFFICIAL  
DEPARTMENT OF THE ARMY POSITION, POLICY, OR DECISION, UNLESS SO  
DESIGNATED BY OTHER DOCUMENTATION.

# **RADIATION CURING OF FABRIC REINFORCED ELASTOMERIC COMPOSITES**

Feng-Jon Chang, Joseph Silverman, and Walter J. Chappas  
Department of Materials & Nuclear Engineering  
University of Maryland, College Park, MD 20742-21150

## **INTRODUCTION**

Ionizing radiation from cobalt-60 gamma and electron beam sources are used to investigate methods to improve the abrasion resistance of polyurethane elastomers. Radiation curing of acrylated urethane oligomers and grafting acrylonitrile onto polyurethanes were studied. Low energy electron beam and plasma surface treatment was also performed. A special device was developed to measure edge abrasion, i.e. the abrasion of folded surface.

Several commercially available acrylated urethane oligomers were cured by radiation. The gel fraction and hardness of cured products were observed to increase with increasing absorbed dose, and abrasion resistance, as well. This indicates abrasion resistance can be improved by increasing crosslink density. However, none of the radiation cured polyurethanes had an abrasion resistance as great as that of the conventional polyurethanes. Surface crosslinking of conventional polyurethane by low energy electron irradiation failed, as did plasma treatment, in the effort to improve edge abrasion resistance.

Far more successful was the graft of polyacrylonitrile on one side of a polyurethane sheet. The polyurethane sheet was immersed in acrylonitrile/n-hexane solution and irradiated by gammas. Variables such as monomer concentration, absorbed dose, and equilibration time were studied. Results show one-side grafting performed in 10 % acrylonitrile/n-hexane with dose 10 kGy could reduce abrasion loss by a factor of two compared to untreated material with significant changes in tensile properties.

## **EXPERIMENTAL**

Acrylonitrile was obtained from Aldrich Chemical Company. It has a boiling point of 77 °C and inhibited by 35-45 ppm hydroquinone monomethyl ether. Conventional polyurethane composites are provided by the U.S. Army Belvoir Research Development and Engineering Center. An oscillatory cylinder abrasive machine used in ASTM D 4157 was modified to measure the edge abrasion property (abrasion on fold) of polyurethane elastomers.



## RESULTS AND DISCUSSION

The one-sided grafted PAN-g-PU sample reveal a 3-region structure: grafted surface; transition region; ungrafted backing. Two surfaces may have different graft content and the core of the sample is virtually ungrafted. In the beginning of the edge abrasion test, only the harder (or more heavily grafted) zone was abraded. After the wearing out of the crest, the softer and harder zones were in simultaneous contact with the abrasive paper. Visual observations show that the size of the debris from the grafted polyurethanes, especially for graft yields larger than 5.9 %, were smaller than the ungrafted ones at the beginning of abrasion. With 5.9 % graft significantly larger debris appear after 100 cycles. The size of debris between 1.5 % grafted and ungrafted polyurethane were indistinguishable. According to Mitsuhashi<sup>1</sup>, the larger debris size indicates a larger abrasion loss. Figure 1 compares the abrasion loss for PAN-g-PU synthesized from 10 % AN/ n-hexane solution with result from different grafts. The abrasion loss seems to level-off for 13.6 % and 20.5% grafted PAN-g-PU. However, shows that the abrasion loss rates in the first 60 cycles are almost identical for both of them, and for a larger cycle number, that the 13.6 % graft lost its weight faster than the 20.5 % graft. This may indicate that both have similar surface graft densities (PAN weight/unit weight of surface) but the depth of the graft is different. The abrasion loss rate decreases with increasing cycle number for 0 % and 1.5 % grafted polyurethanes; this is probably due to the protection by the debris. On the other hand, for other PAN-g-PU's, the abrasion loss rate increases in the cycle range of 60 - 100. This is the effect of change in the graft density in overcoming the effect of debris protection; and after 100 cycles, debris protection becomes stronger. The elastic moduli of the grafted (up to 10 kGy) and untreated PU differ less than 10 %.

## CONCLUSIONS

This work demonstrated that radiation grafting techniques are an effective technique for improving the edge abrasion resistance of polyurethane, with minimal changes in the bulk mechanical properties. Best properties were observed in 10% AN/n-hexane solution irradiated to a 10 kGy absorbed dose.

## REFERENCES

1. K. Mitsuhashi and H. Kaidou, Nippon Gomu Kyokaishi, 68, 497 (1995)

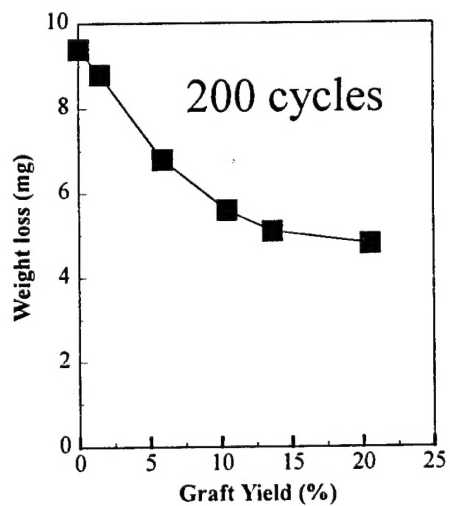
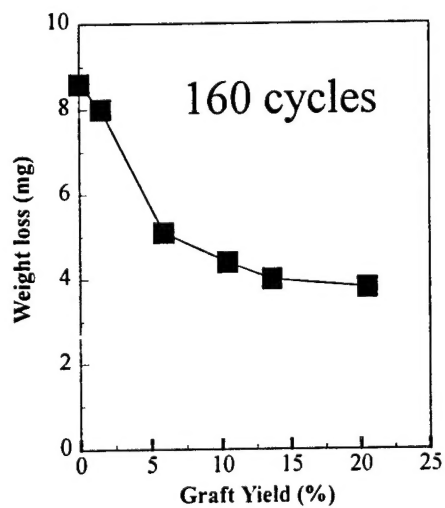
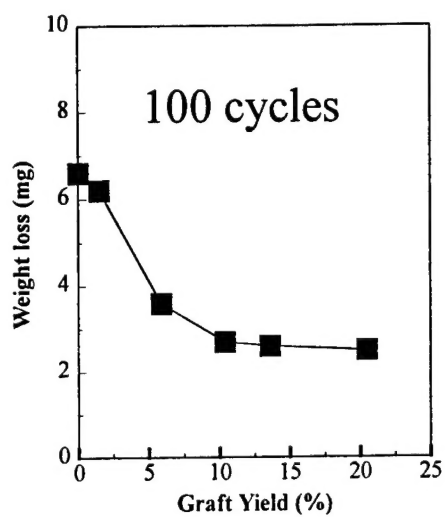
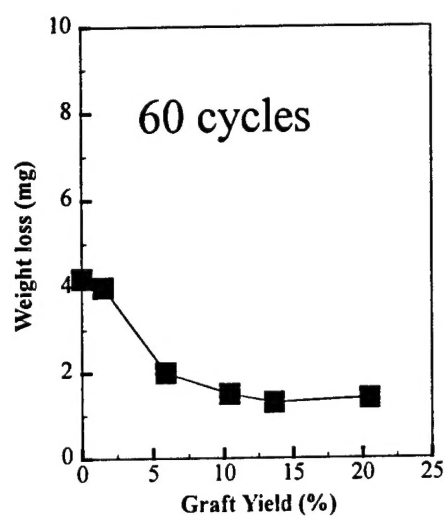


Figure 1. Fold-abrasion loss as a function of acrylonitrile graft.

**ABRASION RESISTANCE OF ELASTOMERS  
MODIFIED BY IONIZING RADIATION**

by

**Feng-Jon Chang**

**Thesis submitted to the Faculty of the Graduate School of the  
University of Maryland at College Park in partial fulfillment  
of the requirements for the degree of  
Master of Science  
1996**

## ABSTRACT

**Title of Thesis:**     **ABRASION RESISTANCE OF ELASTOMERS  
MODIFIED BY IONIZING RADIATION**

**Degree candidate:**   **Feng-Jon Chang**

**Degree and year:**    **Master of Science, 1996**

**Thesis directed by:** **Professor Joseph Silverman  
Department of Materials & Nuclear Engineering  
University of Maryland, College Park, MD 20742-2115**

Ionizing radiation from cobalt-60 gamma and electron beam sources are used in this work in order to investigate methods to improve the abrasion resistance of polyurethane elastomers. Radiation curing of acrylated urethane oligomers and grafting acrylonitrile onto polyurethanes were studied. Low energy electron beam and plasma surface treatment was also performed. A special device was developed to measure edge abrasion, i.e. the abrasion of folded surface.

Several commercially available acrylated urethane oligomers were cured by radiation. The gel fraction and hardness of cured products were observed to increase with increasing absorbed dose, and abrasion resistance, as well. This indicates abrasion resistance can be improved by increasing crosslinking density. However, none of the radiation cured polyurethanes had an abrasion resistance as great as that of the conventional polyurethanes. The attempt to achieve heavy surface crosslinking of

conventional polyurethane in order to improve edge abrasion resistance by low energy electron irradiation failed as plasma treatment.

For more successful in improving edge abrasion resistance was the graft of polyacrylonitrile on one side of a polyurethane sheet. The grafting of polyacrylonitrile onto polyurethane was done in acrylonitrile/n-hexane solution. Variables such as monomer concentration, absorbed dose, and equilibration time were studied. Results show one-side grafting performed in 10 % acrylonitrile/n-hexane with dose 10 kGy could reduce abrasion loss by a factor of two compared to untreated material with minor changes in bulk properties.

# **ABRASION RESISTANCE OF ELASTOMERS MODIFIED BY IONIZING RADIATION**

by

**Feng-Jon Chang**

Thesis submitted to the Faculty of the Graduate School of the  
University of Maryland at College Park in partial fulfillment  
of the requirements for the degree of  
Master of Science  
1996

## **Advisory Committee:**

**Professor Joseph Silverman, Chairman / Advisor**  
**Professor Theodore G. Smith**  
**Professor Nam Sun Wang**  
**Professor Raymond A. Adomaitis**

## ACKNOWLEDGMENTS

In the beginning, I would like to express my deepest appreciation to my dear and erudite advisor Professor Joseph Silverman for his kindly and tireless instruction. Without him, my writing would not have become a thesis.

Great thanks to Professor Theodore Smith for his support and suggestions. I extend my sincere appreciation to Dr. Walter Chappas, thank him for his inspired ideas and for serving as a bridge between me and the radiation industries.

I also want to thank all the staffs in the Radiation Facilities, to Mr. Vincent Adams and Mr. Jeffrey Banta for their assistance in LINAC irradiations, and to Mr. Steve Petras for his assistance cobalt-60 gamma irradiations.

Special thanks go to my partners in the Laboratory for Radiation and Polymer Science (LRPS), starting with Ms. La Rhonda Borum (best wishes to her baby), Mr. Ruoh-Haw Chang, Ms. Mahnaz Chaychian, Mr. George Prieto, Mr. Siddharth Chhabria, Mr. Bryan Berry, and Mr. Ayal Snir for their help and encouragement.

This research was performed under the sponsorship of U.S. Army Research Office whose financial support is gratefully acknowledged.

Appreciation is also extended to Ms. Dawn Crawford of the Belvoir Research Development and Engineering Center for the supply of materials and for the instruction on the basic concepts in polyurethanes; to Professor Ira Block for his kindly donation of an abrader; to Professor Robert Briber, Drs. Eli Golfeiz and Otto Wilson for their helpful suggestions; to Dr. Ming C. Shen for his instruction in tribology; to

Mr. Yi-Hung Lin for his instruction in the operation of Sintech 20; to Mr. Keith Rogers for his instruction in TMA operation; to Dr. Sam Nablo of EPS Inc. for low energy electron irradiation; and to Mr. Keith Neider of InPro Inc. for plasma treatments.

At last, I would like to attribute all my honors to my parents, without their unconditional support and endless love, I could not have come here and continue my academic works.



# TABLE OF CONTENTS

List of Tables.....	vi
List of Figures.....	vii
<b>1 Introduction.....</b>	<b>1</b>
<b>2 Theoretical Background.....</b>	<b>3</b>
2.1 Polyurethane elastomers.....	3
2.2 Acrylated Urethane Oligomers and Polymers.....	3
2.2.1 Structure of Urethane Acrylates.....	3
2.2.2 Reactive Diluents.....	5
2.2.3 Curing of UA.....	5
2.2.4 Morphology of UA.....	6
2.2.5 Mechanical Properties.....	8
2.2.6 Glass Transition Temperature.....	10
2.3 Thermal Degradation of Polyurethanes.....	11
2.4 Photodegradation of Polyurethanes.....	14
2.5 The Wear of Polymeric Materials.....	17
2.5.1 Review of Studies on the Wear of Polymers.....	18
2.5.1.1 Rigid Polymers.....	19
2.5.1.2 Elastomers.....	21
2.5.1.3 The Wear of Polyurethane.....	26
2.6 Graft Copolymers.....	29
<b>3 Experimental.....</b>	<b>31</b>
3.1 Raw Materials.....	31
3.2 Special Instrument for Measuring Edge Abrasion.....	31
3.3 Irradiation of Urethane Oligomers.....	36
3.3.1 Electron Beam Irradiation.....	36
3.3.2 Gamma Ray Irradiation.....	36

3.4 Grafting.....	37
3.5 Gel Fraction.....	38
3.6 Hardness.....	38
3.7 Low Energy Electron Bombardment.....	39
3.8 Plasma Treatment.....	39
3.9 Mechanical Properties.....	39
<b>4 Results and Discussions.....</b>	<b>40</b>
4.1 Abrasion Tests.....	40
4.1.1 Variables in Abrasion Test.....	40
4.1.2 Abrasion Loss in Different Sides.....	46
4.2 Polyurethane from Irradiation Curing.....	47
4.2.1 Gel Fraction.....	47
4.2.2 Abrasion Loss.....	48
4.2.3 Hardness and abrasion Loss.....	52
4.3 Surface Treatment by Low Energy Electron Beam.....	55
4.4 Surface Treatment by Plasma.....	57
4.5 Polyacrylonitrile Grafted Polyurethane (PAN-g-PU).....	58
4.5.1 Nature of Graft.....	58
4.5.2 Graft Yield.....	59
4.5.3 Abrasion Loss.....	66
4.5.4 Heat Treatment.....	70
4.5.5 Grafting and Changing Bulk Properties.....	73
4.5.5.1 Surface Grafting.....	73
4.5.5.2 Choice of Grafting Conditions.....	76
4.5.5.3 Graft on One Side.....	76
4.5.5.4 Mechanical Properties.....	78
4.5.5.5 Effect of Dose Rate.....	
4.5.5.6 Permeation and Chemical Resistance.....	79
<b>5 Conclusions and Accomplishments.....</b>	<b>80</b>
<b>Reference.....</b>	<b>82</b>

## LIST OF TABLES

1	Various structures of hydroperoxides in polyurethane.....	14
2	Abrasive papers used and the corresponding values of hardness and grain size.....	41
3	The graft conditions and yields of PAN-g-PU.....	61
4	Graft conditions and yields of PAN-g-PU in the 10 % AN/n-hexane solution.....	62
5	The comparison of acrylonitrile intake and graft yield.....	63
6	The swelling data of PAN-g-PU.....	64
7	The swelling of polyurethane in the different solution systems.....	65
8	The comparison of abrasion loss for PAN-g-PU before and after heat treatment.....	72
9	Graft condition.....	73
10	Graft yields of one side grafted PAN-g-PU.....	76
11	Modulus of grafted and ungrafted polyurethane.....	78

## LIST OF FIGURES

1	Oscillatory Cylinder Abrasive Machine.....	33
2	Schematic diagram of Oscillatory Cylinder Machine.....	34
3	Method to make specimen set.....	35
4	The arm of load set.....	35
5	Sample holder for curing of urethane oligomers.....	37
6	geometry of abrasive and abraded surfaces.....	43
7	Abrasion loss vs. cycles for the PU sliding against SiC abrasive papers with different grain sizes.....	44
8	Abrasion loss vs. cycles for the PU sliding against abrasive papers with the same grain size but different grinding materials.....	44
9	The shape of the specimen at different times.....	45
10	Gel fraction vs. doses for EB cured urethane oligomers.....	49
11	Shore A hardness of cured CN980M50 at different doses.....	49
12	Gel fraction vs. doses for CN980M50 cured by gamma ray irradiation.....	50
13	Shore A hardness of CN980M50 cured by gamma ray irradiation.....	50
14	Abrasion loss vs. cycles for cured CN980M50 with different gel fractions.....	51
15	Abrasion loss rates for cured CN980M50 with different gel fractions at different cycle ranges.....	51
16	The relation between shore A hardness and gel fraction for the cured CN980M50.....	54
17	Abrasion loss vs. hardness for the cured CN980M50 after 20 cycles.....	54

18	Abrasion loss of PU with low energy EB treatment.....	56
19	Abrasion loss of plasma-treated PU.....	57
20	PAN-g-PU in THF.....	60
21	The swelling of PU (wt. %) in different concentration of AN/n-hexane solution (vol. %)......	61
22	The relation between graft yields and doses for PAN-g-PU.....	62
23	The abrasion scheme of PAN-g-PU.....	67
24	Abrasion loss of PAN-g-PU synthesized from 10 % AN/n-hexane with different graft yields.....	68
25	Abrasion loss rate of PAN-g-PU.....	69
26	Crosslinking of polyacrylonitrile.....	71
27	The comparison of abrasion loss for PAN-g-PU with similar overall graft yield but synthesized from different monomer concentrations.....	75
28	The abrasion loss rate for PAN-g-PU with similiar overall graft yield but synthesized from different monomer concentrations.....	75
29	Abrasion loss vs. graft yield for one side grafted PAN-g-PU.....	77
30	Abrasion loss of PAN-g-PU synthesized from different dose rates.....	80
31	Abrasion loss rate of PAN-g-PU synthesized from different dose rates.....	80

# CHAPTER 1

## INTRODUCTION

Polyurethane (PU) elastomers can provide abrasion-, weather-, fuel-, tear-, and water-resistant coatings for high performance fabrics [1]. A polyurethane-coated nylon fabric has been used by the United States Army as material for collapsible fuel and water tanks. Although polyurethane elastomers have been found to have better abrasion resistance than other elastomers, severe abrasion losses which happen on the folded edge (edge abrasion) of the tanks during shipment cause their failure.

The purpose of this work is first to develop a reliable device to measure edge abrasion resistance. Then, after studying the theories related to abrasion properties by reviewing literature, series of experiments were designed to improve the abrasion resistance of polyurethane materials: (1) polymerization of commercial available acrylated urethane oligomers by ionizing radiation as replacements of conventional materials, (2) surface treatment of conventional polyurethane by low energy electron bombardment, and (3) grafting of polyacrylonitrile onto the surface of conventional polyurethane.

The problems of edge abrasion (abrasion on fold), have been known for many years. However, there is neither a standard and ASTM method nor any published procedure for measuring edge abrasion loss. The first goal of this investigation is to

create a device and a procedure for measuring the edge abrasion loss by modifying an oscillatory cylinder abrasive machine we have in hand.

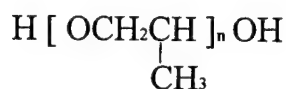
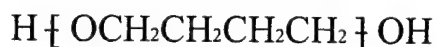
Ionizing radiation has been widely used in curing the coatings, modifying the properties of polymers by crosslinking or scission, and as a means of grafting monomers into the polymer chains. These processes involve the absorption of massive doses to the polymer or polymer-monomer system. Two types of ionizing radiation, cobalt-60 gamma (about 1.25 MeV) and electrons with energies 0.25 - 10 MeV are the most common industrial sources [2]. The use of ionizing radiation (both cobalt-60 and electron beam) in the bulk polymerization of urethane acrylate oligomers, and surface modification of polyurethane by grafting as well as low energy irradiation surface treatments in order to increase abrasion resistance was investigated in this work.

## CHAPTER 2

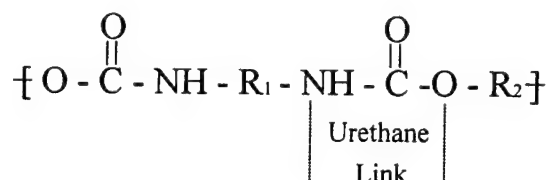
### THEORETICAL BACKGROUND

#### 2.1 Polyurethane Elastomers

Polyurethane elastomers belong to a class of polymers termed "linear segment polymers." Linear segmented polyurethane elastomers consist of a long rubbery soft segment, generally based on hydroxyl terminated polyester or polyether, and a shorter rigid hard segment, generally based on an isocyanate and short chain diol.



(A)



(B)

**Scheme 1.** Examples of (A) soft segments and (B) hard segments of polyurethane.

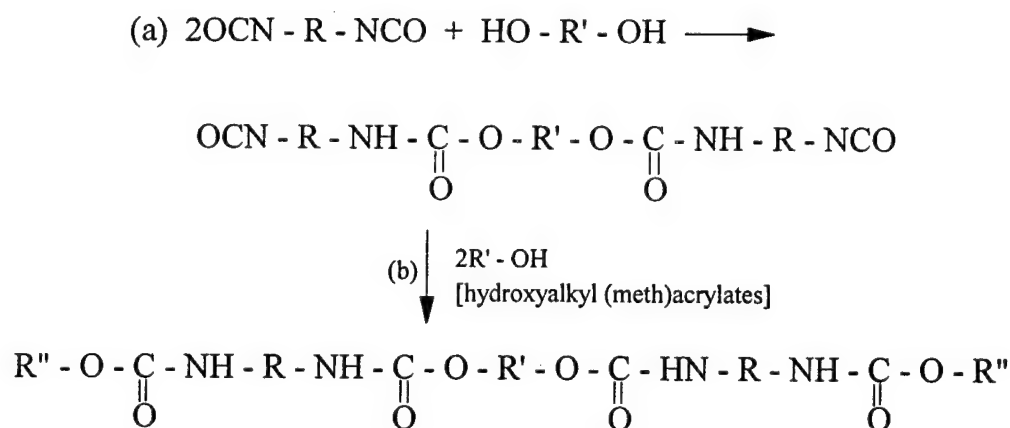
#### 2.2 Acrylated Urethane Oilgomers and Polymers

##### 2.2.1 Structure of Acrylated Urethane

Urethane acrylate (UA) oligomers have been extensively investigated as protective coatings which are cured by steady state or pulsed light sources or by



ionizing radiation (electrons or gamma rays). The basic elements of the resins are urethane oligomers containing acrylic functionality and vinyl monomers which are added to make harder products and/or to reduce the viscosity of the precursor liquid for better processability [3]. The starting material for the urethane oligomers is a polyether or polyester macroglycol having a low glass transition temperature,  $T_g$ . The polyester segments are responsible for toughness, abrasion resistance, high tear strength, and resistance to ozone, and UV light, and also impart polarity to the resin; the polyethers impart good low temperature properties, hydrolytic stability, and resistance to fungal attack. However, polyether segments are more susceptible to oxidative attack and degradation upon UV exposure [2, 4]. The reaction scheme for the synthesis of UA shown in **Scheme 2** involves preparation of (a) isocyanate-terminated macroglycol and (b) acrylate-end-capped urethane oligomers [4].



**Scheme 2.** Synthesis of UA.

### 2.2.2 Reactive Diluents

Reactive diluents such as monofunctional N-vinyl pyrrolidone (NVP) [5-8], difunctional hexanedioldiacrylate (HDDA) [9,10], and trifunctional trimethylol propane triacrylate (TMPTA) [11-13] can be primarily added to UA to control the viscosity and to improve processability, strength, elongation, chemical and scratch resistance, and surface finish, and to control the crosslink density. Ideal reactive diluents require low viscosity, good solvent power, high cure rate, low toxicity, low odor, and desired physical characteristics after curing. The effects of several different diluents on the properties of Uvithane (urethane oligomers made by Thiokol Co.) have been reported [14].

### 2.2.3 Curing of UA

The olefinic double bond present at the chain ends of UA can be polymerized by thermal and free radical initiators, as well as by exposure to electron beam (EB), gamma, ultraviolet, laser, and radiation of longer wavelength such as infrared and microwave [4].

EB curing proceeds, in general, by a free radical mechanism, and the steady state reaction rate,  $R_p$  can be express as

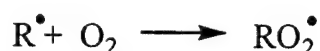
$$R_p \propto \dot{D}^{1/2} [M]$$

where  $\dot{D}$  is the absorbed dose rate and  $[M]$  is the oligomer concentration [15]. Lower concentration of double bonds and higher viscosity reduce the reaction rate [15] and affect the dependence on  $\dot{D}$  as well as the molecular weight of the polymer.

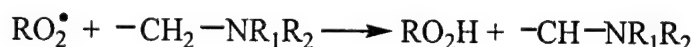
The advantage of using high energy radiation over chemical initiators to cure urethane acrylate oligomers is that no decomposition products of the initiators are

formed. The crosslink density of EB-cured gel film, as evaluated by the average molecular weight between crosslinking junctions, increases steeply up to 50 kGy; only a marginal increase occurs with any further increase in dosage [16]. This may be due to crosslinking through terminal acryloyl double bonds at doses less than 50 kGy. At higher doses the crosslinking may be related to the polymer backbone.

The existence of oxygen is found to inhibit curing compared to curing in nitrogen atmosphere because oxygen reacts with radicals, i.e.,



The peroxy radical formed is long-lived and is not an effective chain initiator unless an effective hydrogen donor like an amine is present. The latter can generate an effective radical via the hydrogen transfer reaction [4].



#### 2.2.4 Morphology of UA

The domain structure that results from phase segregation of the hard and soft segments in polyurethane is well recognized as the principal feature controlling the properties of this class of elastomers [17]. It is recognized that a wide variety of variables, such as the type of hard and soft segments, molecular weight, and molecular weight distribution of the two components, the chain extender, the stoichiometric ratio between them, the processing history, and the polymerization method all affect the degree of phase separation, the hard segment domain size and, accordingly, the bulk and surface properties of the polymers [18-21].

Wadhwa and Walsh studied the morphology of EB-cured UA based on TDI (toluene-diisocyanate)-HEA (2-hydroxyethyl acrylate) [22] and TDI-HEMA (2-hydroxyethyl methacrylate) [23] oligomers. Only one value of  $T_g$  was found for each film indicating that the hard and soft segments are mixed homogeneously. The films obtained from hard-segment rich oligomers are hard and somewhat brittle, they exhibit one-phase morphology in which hard glassy segments play a dominant role. The films are soft and tough when soft rubbery segments are more prominent. The heterogeneous structure of interpenetrating networks based on UA was studied by Shilov et al. [24] using small-angle x-ray scattering. Lin et al. [25] found a small amount of a separate UA phase caused by increasing polyol molecular weight. The relative hydrogen bond concentration detected by Fourier transform infrared spectroscopy (FTIR) has been used to find evidence of phase separation [26, 27].

Ando and Uryu [28] irradiated semicrystalline urethane oligomers at different temperature. They found that if EB polymerization takes place below the  $T_m$  of the prepolymer, semicrystalline UA with a spherulitic structure is obtained. On the other hand, EB polymerization above  $T_m$  destroys the crystalline phase of the prepolymer to give transparent gel films. They also found that the film from 100 kGy of EB irradiation at 25 °C has higher crystallinity and larger crystallite size than the film from UV irradiation. The reason is that EB irradiation below the melting point of the polyurethane acrylate can lead to crosslinking without the destruction of the original crystalline structure while the UV polymerization proceeds with the melting of the

crystalline structure by absorbing lights other than the UV absorbed by the photoinitiator.

### **2.2.5 Mechanical Properties**

The ratio of hard-to soft segments in UA, the concentration and nature of the reactive diluent, the molecular weight of UA prepolymer, and the curing technique affect the tensile properties of cured UA. Larger hard-to-soft segment ratios and higher crosslink densities give films with a higher modulus [29]. Schmidle [14] observed, on the addition of benzyl acrylate as a reactive diluent, an increase in elongation at break and a decrease in modulus with no change in tensile strength. However, lower elongation and higher modulus are the results of the addition of HDODA, TMPTA, and NVP. Several authors [31-34] have investigated the effects of reactive diluents on the mechanical properties of cured films. Films made with an added multifunctional diluent generally have a higher tensile strength of cured films and lower elongation at break than cured films from a neat oligomer [32, 33]. On the other hand, a monofunctional diluent, generally speaking, reduces the tensile strength and enhances the elongation of polymers. However, NVP has been found to enhance both the tensile strength and elongation by adding it to acrylated urethane oligomers [30-32,34]. Levy and Massey [35] used two monofunctional diluents, NVP and EOEOEA in different concentrations. They showed that EOEOEA undergoes homopolymerization and does not become a part of a crosslinked network, thereby resulting in a decrease in modulus, tensile strength, and elongation. In this case, EOEOEA acts similar to a compatible plasticizer.

The effect of polyol molecular weight (MW), polyol type, and reactive diluent content on the mechanical properties of IEM and TDI-HEMA [25] have been reported. These studies indicate that the polyol primarily affects the room temperature modulus due to differences in the position and breadth of the polyol  $T_g$ . Increasing polyol MW leads to a lower polyol  $T_g$ , a smaller amount of a separate urethane acrylate phase and a larger chain length between crosslinks. The first two effects are reflected in lower modulus and strength at room temperature, while a larger chain length between crosslinks leads to higher elongation at break at room temperature and lower modulus at high temperatures. Li et al [36] found the crosslinking process of UA depress crystallization of the soft segments and improves tensile properties.

Ando and Uryu studied the effect of polymerization temperature [37], irradiation dose [16], prepolymer MW [38] on the radiation-cured film. They observed that increasing the irradiation dose increases the gel fraction, opacity, and tensile strength, whereas elongation at break remains constant. Stress at yield and modulus reaches a maximum at 25 kGy and then decreases with increasing dose. The gel film cured below the melting temperature of the crystal,  $T_m$ , has higher values of stress at yield, Young's modulus, and tensile strength than those cured above  $T_m$ . Young's modulus, tensile strength, and elongation at break show minimum values at a prepolymer MW of 1700; and they increase with increasing MW. Idriss Ali et al. [39] examined several mono-, di-, and tri-functional reactive diluents on the properties of UV cured film. They found reactive diluents with trifunctional acrylate groups that

have a branching effect can yield more crosslinking in the cured film; however, the tensile strength is not always enhanced.

### 2.2.6 Glass Transition Temperature

In general, the  $T_g$  of the rigid segments is from 30 °C to 200°C and the  $T_g$  of the flexible segments is commonly -90 to -80 °C for polyetherurethanes and -45 to -12 °C for polyesterurethanes [40]. As the flexible segments become longer, the  $T_g$  of the polyurethanes decreases asymptotically.

In the solid state, at room temperature, all the N-H groups in polyesterurethanes and polyetherurethanes groups are hydrogen bonded [41]. In polyesterurethanes, the hydrogen bonds of the NH groups with the urethane C=O groups (ca 60%) and with their ester analogues (ca 40%) are dispersed throughout the polymer bulk [42]. In polyetherurethanes the stronger N-H...O=C hydrogen bonds, with an equilibrium constant for bond formation ca 3, are sometimes diluted several times with a large number of the NH...O< with a bond formation constant of 0.5. In polyetherurethanes, 85% of NH groups are hydrogen bonded, and of that number 38% are bonded with C=O and 62% with ether groups [43]. The more C=O groups that are hydrogen bonded, the higher the melting point of the rigid segments, and the lower the  $T_g$  of the flexible segments [44].

The effect of diluent content on the properties of UA has been reported [3, 32]. For one-phase materials, increasing NVP content results in an increase in the  $T_g$ . For two-phase materials, increasing NVP contents increase the  $T_g$  of the hard segments while the  $T_g$  of the flexible segments is unaffected. Dai et al. added reactive diluents

(20% NVP or DEGDA) to the IPID-HEMA-PPO system which caused a slightly higher  $T_g$  of the PPO [45] due to a higher crosslinking density and an energy barrier to the movement of chain segments with added reactive diluents.

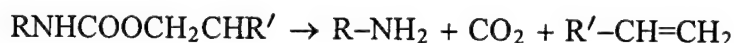
## 2.3 Thermal Degradation of Polyurethanes

The urethane linkage has moderate thermal stability; the decomposition temperature is between 150 and 250 °C [40]. Thermal degradation involves random scission, depolymerization, termination and chain transfer reactions. Studies of the thermal decomposition of substituted urethanes show that the three general reactions in the **Scheme 3** take place [45, 46].

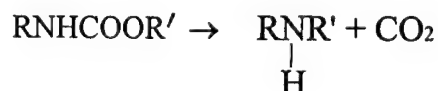
**Dissociation to isocyanate and alcohol:**



**Formation of primary amine and olefin:**



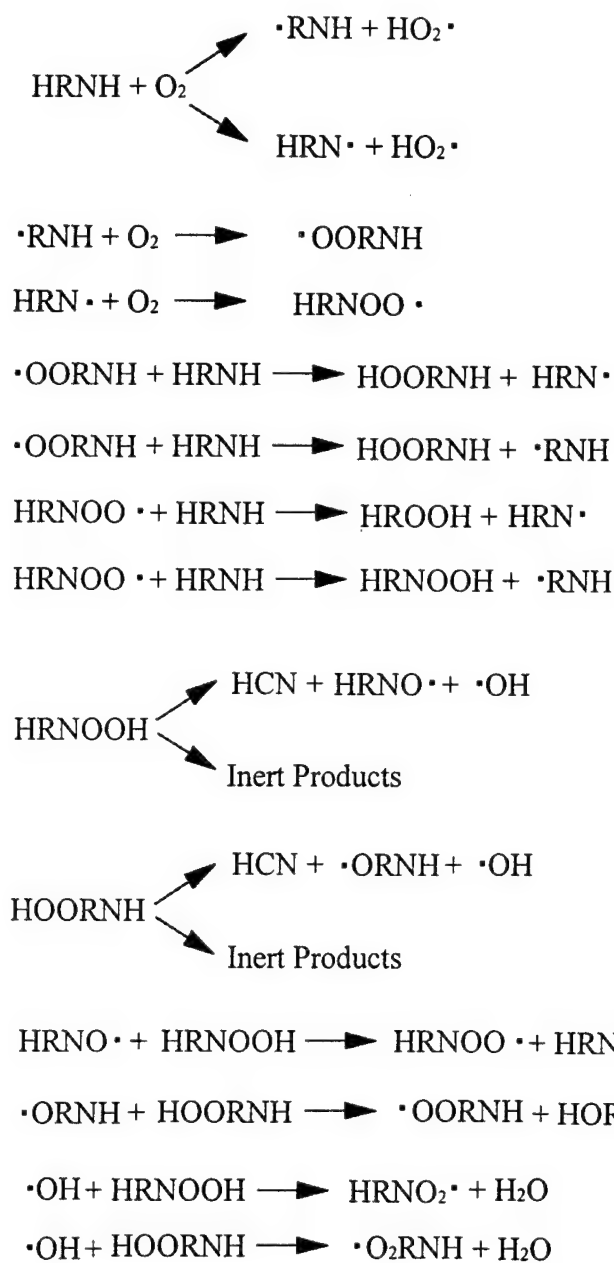
**Formation of secondary amine:**



**Scheme 3.** Thermal decomposition of polyurethanes.



According to Jellinek and Dunkle [47], the thermal degradation process of polyurethane under oxidative conditions proceeds at elevated temperature according to the radical mechanism shown on **Scheme 4**.



**Scheme 4.** Thermal degradation process of polyurethane under oxidative conditions.

## 2.4 Photodegradation of Polyurethanes

The photodegradation of polyurethanes occurs through urethane group scission (**Scheme 5**), which is more pronounced in polyester based polyurethanes, and through the ether group scission in polyether based polyurethanes (**Scheme 6**) which results in formation of hydroperoxides at the carbon atoms adjacent to the ether linkage (**Table 1**, type (B)) [48-51].

The rate of yellowing is faster in polyesterurethane, but it does not correlate with the intensity of oxidative degradation. It is connected with the transformation from aromatic to the quinoid structures which is the radiation initiated degradation of aromatic isocyanate based urethanes. This transformation occurs via hydroperoxides of type (A) (**Table 1**). In polyetherurethane, hydroperoxide of type (B) (**Table 1**) is formed. In polyesterurethane the hydroperoxides is also formed from the  $-\text{CH}_2-$  group of the ester group (**Table 1**, type (C)) [48-52].

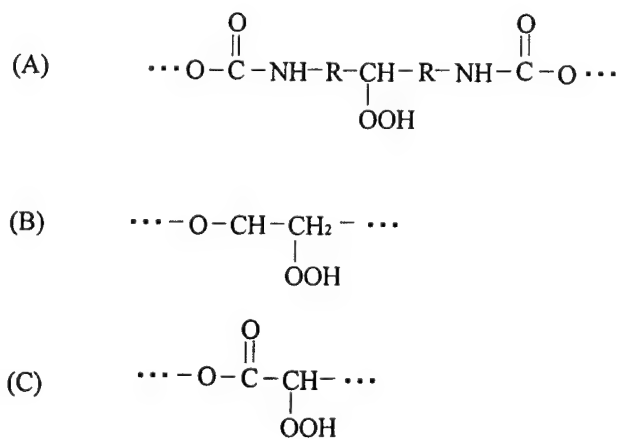


**Table 1.** Various structures of hydroperoxides in polyurethane.





## 2.5 The Wear of Polymeric Materials

Wear can be defined as the progressive loss of materials from the surface of a body as a consequence of relative motion. Three primary processes are involved: deformation of the surface asperities to support the load; detachment of material from the surface; and removal of this detached material from between the contacting surfaces as loose debris [53]. One of the classifications of the various types of wear is as follows [54]:

(1) Abrasive wear: caused by the presence of hard asperities on one or both surfaces, by the presence of hard particles between the surfaces, or by hard particles embedded in one of them. The cutting action of the particles is usually a major component.

(2) Erosive wear, or erosion: caused by relative motion between solid particles entrained in a fluid. When the relative motion of the particles is more or less parallel to the surface, wear is called abrasive erosion, and when nearly normal to the surface, impingement erosion.

(3) Fatigue wear: the detachment of particles as a result of cyclic stress variations. It is usually associated with rolling, but localized fatigue on an asperity scale is becoming increasingly recognized as a factor in sliding wear, too.

(4) Corrosive wear: a process in which chemical reaction with the environment is the rate-determining factor. An alternative term is oxidative wear, when oxygen is the primary reactive element involved.

(5) Adhesive wear: the transfer of material from one surface to another during relative motion as a consequence of adhesive forces. The transferred fragments may be either permanently or only temporarily attached to the other surface.

The nature of the wear mechanism can be determined from a scanning electron microscopic (SEM) examination of the wear surface. Abrasive wear is indicated by cutting or gouging marks on the surface. Fatigue wear leads to the formation of cracks on the surface and the removal of relatively large chunks of the surface in regions that have been surrounded by intersecting cracks. However, in practice, the wear process occurring with any given combination of materials frequently involves a combination of several types of wear. Fatigue, for instance, may play a significant part in the abrasive wear of rubbers, and in the adhesive wear of rigid polymers [53].

### **2.5.1 Review of Studies on the Wear of Polymers**

Selwood [54] made an interesting contribution to the problem of developing a relationship between abrasion and other physical properties applicable to many diverse materials. At a given hardness, more extensible (ductile) materials are more abrasion resistant. Glaeser [55] suggested as a rule of thumb that the wear rate of polymeric compositions are directly proportional to the load applied to the material, and inversely proportional to its tensile strength when the test specimens are at a comparable condition of surface roughness and surface temperature.

### 2.5.1.1 Rigid Polymers

A simply theory of abrasive wear can be developed by assuming that a hard conical asperity indents a softer material and plows or cuts a groove during sliding. This leads to the relationship [56]

$$V = K \frac{Ld \tan \theta}{\pi H} \text{ or } W_d = \frac{KL \tan \theta}{\pi H}, \quad (1)$$

where  $W_d = V/d$ ,  $V$  is the volume removed,  $d$  is the distance of sliding,  $\theta$  is the angle of slope of the cone,  $L$  is the load and  $H$  is the indentation hardness of the soft material. The constant factor  $K$  expresses the fact that not all material in the groove is removed as debris, and some is merely displaced plastically. A similar result holds for a surface model involving sharp ridges; in this case,  $K = 2$ .

Oberle [57] has suggested that the ratio  $H/E$  ( $E$  = Young's modulus), which defines the elastic limit of strain, is more relevant to the abrasive wear. Ratner et al. [53] have examined the importance of the elongation at break as a factor in the abrasive wear process. They claimed that the production of a loose wear particle involves three stages: (1) deformation of the surfaces to an area of contact determined by the hardness  $H$ , (2) relative motion opposed by a frictional force  $F = \mu L$ , and, finally, (3) disruption of the material at the contact points involving an amount of work equal to the integral of the stress-strain relationship, or approximately equivalent to the product of the breaking stress  $S$  and the elongation at break  $\epsilon$ . Thus, the volume worn per unit distance of sliding,  $V/d$ , is proportional to  $1/H \times \mu L \times 1/S\epsilon$  and the specific wear rate is



$$W_L = \text{Const.} \frac{\mu}{HS\epsilon} \quad (2)$$

where  $W_L = V/dL$ . The absolute magnitude of the predicted wear rates would, however, change appreciably. In point of fact, the dominant part in the wear process appears to be played by the product  $1/S\epsilon$ . However, for a series of  $\gamma$ -damaged polytetrafluoroethylenes (PTFEs), Briscoe et al. [58] found that the wear rates against abrasive paper increased less rapidly than proportionately with  $1/S\epsilon$ , or even with  $1/S^2\epsilon$  where the extra  $S$  was introduced as an approximation for the hardness. To explain this trend, they modified the original Ratner argument and introduced an extra term, the damage efficiency, to account for the fact that only some of the strain at rupture is involved in particle detachment and a significant part can be recovered elastically. The damage efficiency term also takes account of the fact that debris within the contact, even during single-pass abrasion, can reduce the effective load and, in turn, the wear rate [59]. In the case of polymer composites under a severe abrasive condition (e.g. abrasion against abrasive paper), Friedrich [60] proposed

$$W_d = \frac{\Psi^*}{H^a} + \frac{\Phi^* H^b}{G_{IC}} \quad \text{with } \Phi^* > 0 \text{ if } p > p_{crit} \text{ and } \Phi^* = 0 \text{ if } p < p_{crit} \quad (3)$$

$$p_{crit} \propto \frac{K_{IC}^2}{H}, \text{ where}$$

$$\Psi^* = \text{Const.} \frac{\mu}{S\epsilon}$$

$\Phi^*$  = a characteristic term of the abrader / wear surface combination.

$p$  = apparent contact pressure.

$p_{crit}$  = threshold value above which wear particles produce detectable microcracking.

$G_{IC}$  = fracture energy

$K_{IC}$  = fracture toughness;  $a = 1$ ,  $b = 1/2$ , and  $c = 1$  in the first-order approximation.

The first term of this equation represents the wear via a plowing process and, the second term, via a microcracking process. Assuming that, for the given testing conditions,  $p \gg p_{crit}$ ,  $W_d$  is mainly characterized by the second term of the equation, and a correlation of the form

$$W_d \propto \frac{H^{1/2}}{G_{IC}} \quad (4)$$

should lead to a good agreement between the experimental wear data and the theory.

### 2.5.1.2 Elastomers

There are three distinct processes can be identified during the sliding of rubbers over hard and abrasive surfaces [61]:

(1) Cutting or tearing produced by asperities with very small apex angles, such as abrasive grains.

(2) Fatigue as a consequence of repeated deformation on surfaces, which are still rough enough to cause high stress concentrations, but do not contain sharp-pointed asperities.

(3) The formation of patterns on the rubber surfaces as a result of high adhesion and frictional forces against both smooth and rough counterfaces.

On sharp tracks such as abrasive paper, various attempts have been made to relate the abrasive wear rates of different rubbers to tensile strength and other mechanical properties. Buist and Davies (1946) have suggested [53]

$$\text{Wear rate} = a_0 - a_1 H_s - a_2 \sigma, \quad (5)$$

where  $H_s$  is the shore hardness,  $\sigma$  is the tensile strength and  $a_0, a_1$  are constants. An alternative relationship has been suggested by Ratner and Klitenik (1959) [53], based on experiments with a variety of vulcanizates of different rubber.

$$W_d = \text{Const.} \frac{\mu(100-D)}{\sigma}, \quad (6)$$

where  $D$  is the percentage rebound resilience, characterizing the hysteresis. Grosch and Schallamach [57] found that the linear rate of abrasion,  $\delta$  is proportional to the normal stress. If abrasion on sharp track is a result of tensile failure, then

$$\delta = \frac{K_1 \mu L}{U} = \frac{2K_1 \mu L}{S\varepsilon}, \text{ and } \delta = \frac{\text{depth of abrasion}}{\text{distance of sliding}} \quad (7)$$

where  $U$  is the energy density at break measured at the appropriate high frequency, and  $K_1$  is a dimensionless constant. Uchiyama [63] proposed

$$\delta = \frac{K_2 L}{ES} \quad (8)$$

It should be noticed that the above equation is not complete, in the sense that  $K_2$  has dimensions. Uchiyama [63] suggested that insertion of  $\varepsilon$  into it spoils the correlation, but Schallamach [64] attributed the observed minimum of  $\delta$  as the temperature is lowered, to the maximum of  $\varepsilon$ .

Thavmani et al. [64] defined abrasability ( $A$ ) as the volume loss per unit friction work, then

$$A = K_3(1/U), \quad (9)$$

where  $U$  is obtained from the area under the stress-strain curve and  $K_3$  is dimensionless. By using a modified Du Pont Abrader, they observed that the abrasability increases linearly with the reciprocal of breaking energy for the individual rubbers: NR, SBR, and HNBR which are both filled and unfilled [66, 67]. The coefficient  $K_3$  represents the volume loss per unit frictional work done on the material for which the breaking energy is unity. The small value of  $K_3$  indicates that only a fraction of the frictional work is utilized in causing rupture and a major part is dissipated. They also found that the abrasion loss decreases with the increase in crosslink density which cause the decrease in hysteresis loss [66]. Moreover, it is known that the breaking energy and the energy loss per unit volume per cycle ( $E_l$ ) are related as follows [67]:

$$U = k(E_l)^{2/3}, \quad (10)$$

where  $k$  is a constant. If  $\epsilon_{1/2}$  is one half of the peak-to-peak dynamic strain and  $E''$  is the loss modulus, then,

$$E_l = \pi \epsilon_{1/2}^2 E''. \quad (11)$$

Because

$$U \sim (E'')^{2/3}, \text{ at constant strain,} \quad (12)$$

or

$$U \sim (G'')^{2/3}, \quad (13)$$

where  $G''$  is the shear loss modulus, therefore

$$A \sim (1/G'')^{2/3}. \quad (14)$$

Mitsuhashi et al. [65] used the Lambourn abrasion test to study which properties of rubber correlate with abrasion but found the physical properties of rubber compound at break and the wear rate are not directly correlated. Paying attention to the relations between the size of particulate wear debris and wear rate, however, they found the following relation:

$$W_t = K_4 \left[ \frac{\Phi}{U} \right]^\alpha \quad (15)$$

where

$W_t$ : wear rate (volume/time)

$U$ : tensile energy density at break

$\Phi$ : area of particulate wear debris

$K_4$ : constant  $\cong 0.006$

$\alpha$ : constant  $\cong 0.4$

There is considerable circumstantial evidence suggesting that particle detachment arises from fatigue during sliding against counterfaces which are insufficiently rough for the elastic limit to be exceeded in asperity deformation.[59]. Reznikovskii has developed a fatigue theory of wear for rubbers based on the assumption that they slide over a rigid counterface on which is superposed a uniform

distribution of hemispherical asperities [53]. In this theory, the fatigue properties of the rubber are characterized by the relationship of the form

$$n = (\sigma_0/\sigma)^b, \quad (16)$$

where  $n$  is the number of cycles to failure at an applied stress of amplitude  $\sigma$ ,  $\sigma_0$  is the ultimate strength of the material in a single application of stress, and  $b$  is a constant characterizing the fatigue properties of the material. It is not easy, however, to decide the point at which the abrasive wear changes to fatigue as the surface topography of the counterface is changed. The mechanisms of two extreme situations, wearing on abrasive paper and wearing against a metal gauze, are considered to be merely abrasive wear and fatigue, respectively. When rubbers are worn on a gauze, the wear rate is no longer proportional to the applied load; instead [53]

$$W_d = K_s L^a, \quad (17)$$

where  $a$  is a constant for a particular material and generally ranges from 1 to 8, it increases as the gauze mesh become finer, and the strength of the molecular interaction measured by cohesive energy density becomes larger. Klitenik and Ratner [53] observed that increasing the polarity of the rubber or the addition of active fillers such as channel blacks results in the increasing of  $a$ , but increasing the degree of swelling of a rubber decreases  $a$ . A direct relationship between  $a$  and the exponent  $b$  in Equation

(16),  $b = (a+2)/3$ , was also proposed. The proportionality constant  $K_s$  represents the volume removed per unit distance of sliding per unit load in the following equation:

$$(K)^\gamma = \text{Const.} \frac{\mu(100-D)}{\sigma_0 E^{\alpha-1} C}, \quad (18)$$

where  $\gamma$  is a constant,  $D$  is the % resilience,  $\sigma_0$  is the tensile strength, and  $C$  is the ratio of the aged to unaged values of the product of tensile strength and elongation at break. The ratio enters because of the breakdown of the surface layers during repeated stressing, when such breakdown does not occur (e.g. sliding on an abrasive paper),  $C = 1$  because the wear rate is sufficiently high to remove the layer as soon as it forms. Since sliding on the abrasive paper  $a = 1$ , **Equation 17** reduces to **Equation 6**.

Although various attempts have been made to relate the wear of elastomers to their physical and mechanical properties, the empirical relationships proposed only have limited applicability. The main reason is that rubber surfaces become extensively degraded during sliding by processes such as chain scission or other free radical reactions; these reactions leads to surface layers whose properties are very different from those of the bulk materials [61].

### 2.5.1.3 The Wear of Polyurethane

Evans and Fogel [70] examined the relationship between the tensile and morphological properties and abrasion resistance of polyurethane films or materials used for floor surfaces. Samples of unspecified composition were placed in a ball mill abrasion tester and subjected to repeated impacts of 14/36 carborundum aluminum oxide and 25 grade porcelain grinding medium. The wear performance was assessed

by determining the 60° gloss reading. No correlation was found between the tensile energy to rupture and abrasion resistance at ambient temperatures. In an attempt to correlate the observed performance, the samples were divided into two arbitrary classes: those with a  $T_g$  above -10 °C and those with a  $T_g$  below this temperature. When the results from samples which remained rubbery at -10 °C were disregarded, some correlation was found between the abrasion resistance and the rupture energy. Samples with low values of rupture energy had the greatest decrease of % gloss. SEM analysis indicated that the more brittle films had failed due to the gouging of the surface by the abrasive media. The films that had glass transitions between -10 °C and room temperature appeared to have failed the gloss test because the surfaces had become crazed. It was thought that as the cracks formed on the surface tensile failure did not occur; however cold drawing at the point of impact was found to lead to the crazing. Materials that remained rubbery below -10 °C which showed no loss of gloss also showed no evidence of cracking or gouging. This was attributed to the fact that the particles did not impact on the surface with enough energy to damage the film.

Li and Hutchings [71] studied the erosion resistance of cast polyurethane elastomers to solid particles. For those polyurethanes with almost the same rebound resilience, there is a trend of increasing erosion rate with increasing hardness, tensile modulus, and tensile strength. The highest resistance to erosion was found in the softest material. Sofuku [72] synthesized polyester and polyether based polyurethanes which have the same isocyanate and changed the length of soft segments. The materials which have a hardness near JIS-A 90° were found to have the best abrasion



resistance. The weight loss seemed to have a minimum value for a certain cohesive energy of molecules; however, this value changes for different types of soft segment.

The relationships between polyurethane chemistry (soft segment molecular weight and hard segment weight percentage) have been studied by Mardel et al. [73] who could not obtain a straightforward relationship. They also concluded that the Ratner-Lancaster correlation (**Equation 2**) only holds for glassy materials and does not hold for elastomeric materials [73]. A comparison was made between the performance of an as-molded thermoplastic polyurethane and one annealed in vacuum for one hour at 155 °C. The wear surfaces were examined by SEM after a Taber Abrader test. The unannealed specimen appeared to have suffered a greater amount of damage with a much rougher and more disturbed surface than the annealed one. The scars on the surface indicated that large sections of the material were removed during the wear test. The gouges traversed the surface of the annealed specimen and plowed the sample to the side of the groove instead of removing those large sections from the surface. The annealed sample with lower initial modulus and greater extensibility appeared to better survive the trauma induced by the wear test. The as-molded samples wear faster because they could not absorb or deflect the energy induced by the wear testing procedure. The improvement in physical properties such as toughness, elongation at break, and stress at break of a commercial thermoplastic polyurethane were found after annealing. However, the authors claimed these improvements do not affect the erosion wear performance remarkably [74]. The major role tends to be played by the morphology changes which include the refining of the domain and the increasing in

interdomain spacings. It should be noted that there is no correlation between wear behavior measured by erosion testing and by a pin or drum abrasive method.

## 2.6 Graft Copolymers

According to the International Union of Pure and Applied Chemistry (IUPAC), graft copolymers are defined as follows [75]: "A graft copolymer is a high polymer, the molecules of a main chain with a particular set of structural units and one or more branches chemically unite. " A simple type of graft copolymer can be represented as follows:



where A and B are different structural units, each deriving from different monomers.

### 2.6.1 Radiation Grafting

The direct grafting method involves the irradiation of a polymeric substrate in the presence of monomers and usually, in the absence of oxygen. Generally speaking, polymers undergoes scission or crosslinking upon irradiation. In the presence of vinyl monomers, the former predominately produces block-type copolymers, and the latter produces a pendant graft structure such as shown above. According to an empirical rule, when each carbon in the main chain of a vinyl polymer carries at least one

hydrogen atom, the polymer crosslinks, and, if a tetrasubstituted carbon is present in the monomer unit, the polymer degrades.

The dose, dose rate of irradiation, diffusion of the monomer into the polymer, and temperature are important factors in the radiation grafting system [76]. The total dose determines the graft yield, usually expressed as a percentage increase in weight, and the dose rate determines the length of the grafted branches. Although conventional homogeneous steady state polymerization kinetics constitute a reasonable approximation and provide an explanation for these effects, the actual detailed mechanism is complex. The monomer diffusion coefficient, the monomer solubility, the monomer concentration in the external solution, and the transfer and termination rate constants of the growing chains affect graft yield.

## **CHAPTER 3**

### **EXPERIMENTAL**

#### **3.1 Raw Materials**

Four urethane acrylate oligomers supplied by Sartomer Inc. are (1) CN 964 neat, a resilient aliphatic urethane acrylate; (2) CN 964E75 blend, an aliphatic urethane acrylate blended with 25% SR-454 (ethoxylated trimethylolpropane triacrylate); (3) CN 980 neat, a fast curing aliphatic urethane acrylate; and (4) CN 980M50 blend, a fast curing aliphatic urethane acrylate blended with 50% SR-339 (2-phenoxyethyl acrylate). CN 964 has a polyester backbone and CN 980 has a polyether backbone.

Acrylonitrile, a highly toxic cancer suspect agent provided by Aldrich Chemical Co. is a liquid with boiling point 77 °C and inhibited by 35-45 ppm hydroquinone monomethyl ether. Conventional polyurethane composites are provided by Ms. Dawn Crawford of U.S. Army Belvoir Research Development and Engineering Center.

#### **3.2 Special Instrument for Measuring Edge Abrasion**

An oscillatory cylinder abrasive machine (**Figure 1, 2**) used in ASTM D 4157 was modified to measure the edge abrasion property (abrasion on fold) of polyurethane elastomers. A sheet of abrasive paper is mounted on the curved surface of oscillating cylinder and fixed to it by edge clamps. Specimens are cut to 2 cm x 1 cm and

clamped to paper clips (Figure 3). The rubber pressure pad (Figure 4) is removed from the pad holder, and a specimen set is stuck onto the inner center surface of the pad holder by a double-face foamed tape. During the measurement, the load set arm is lowered and the specimen is in touch with the surface of the sandpaper. The position of a pressure scale weight on the pressure rod determines the specific load. In order to allow the pressure bar to rest in a horizontal position, the knurled screw on the top of the overarm is adjusted according to the thickness of the specimen. The drum is oscillated 90 cycles per minute for double rubbing. The abrasion section oscillates through an arc of 76 mm. Abrasive paper is replaced after each run. Only one of the four load set arms was used and at least 5 specimens were tested for each test condition. In order to minimize the influence of the environment, all of the specimens tested were dried in a 80 °C vacuum desiccator for 24 hours after washing with n-hexane, then placed in a dry-seal vacuum desiccators until being tested. The abraded specimens also followed the same processes described above before being weighed. Dried calcium chloride pellets were put into a beaker which were placed in the cabinet containing the balance.

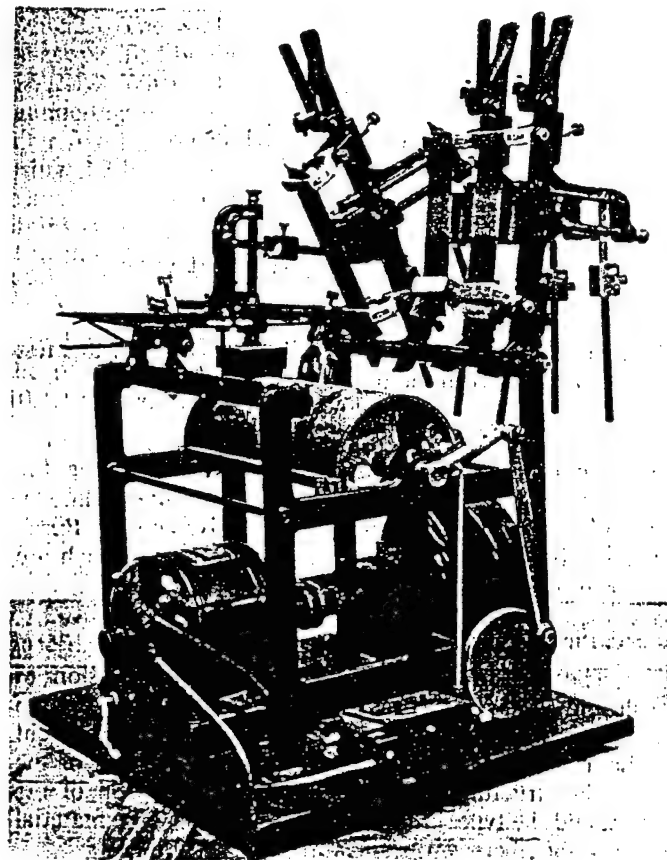


**Figure 1.** Oscillatory Cylinder Abrasive Machine.

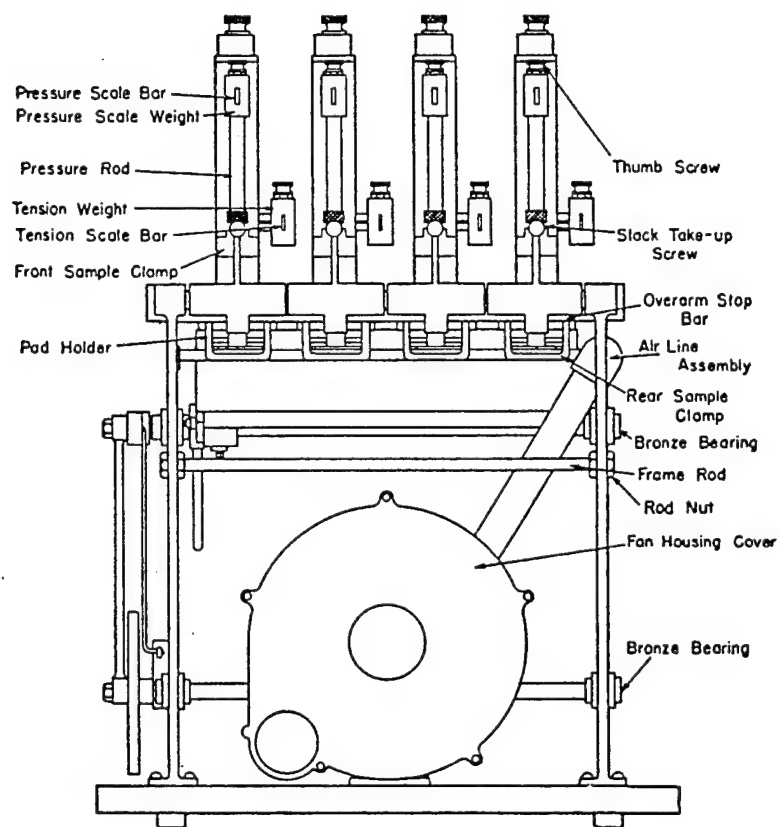


**Figure 2.** Schematic diagram of Oscillatory Cylinder Abrasive Machine.

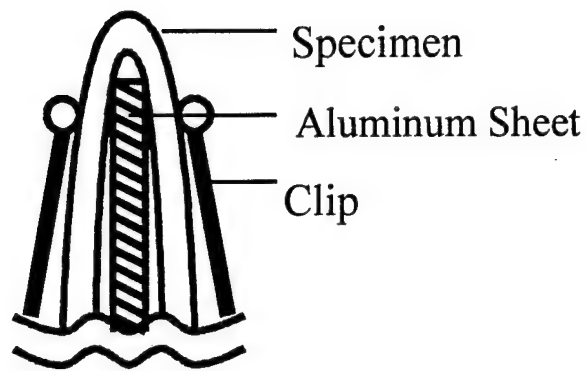


Figure 3. Method to make specimen set.

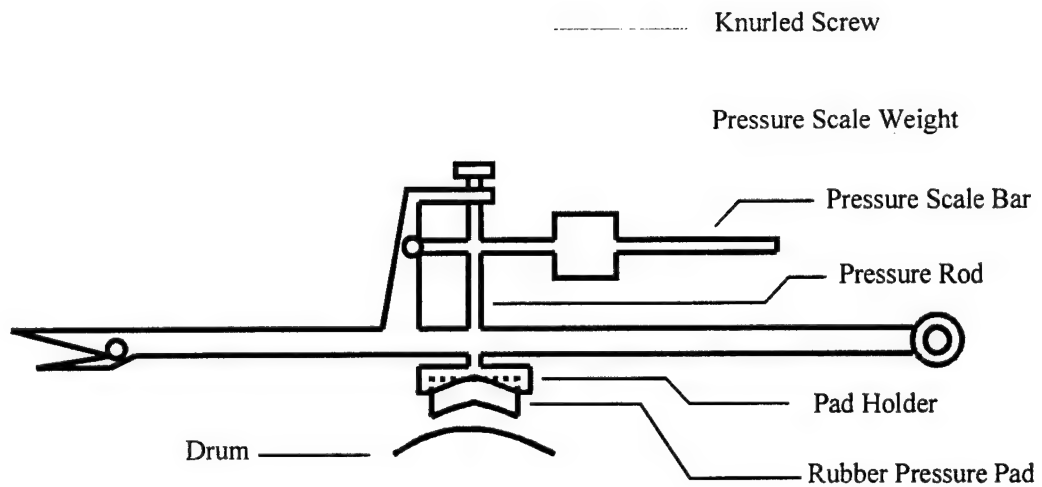


Figure 4. The arm of load set



### **3.3 Irradiation of Urethane Oligomers**

#### **3.3.1 Electron Beam Irradiation**

A sample holder (**Figure 5**) was made by sticking a closed loop of cable (3 mm diameter) onto a 16 cm x 16 cm aluminum plate by chemical adhesive. Urethane oligomer was heated to 70 °C to reduce its viscosity and poured into the volume contained by the loop and the plate. Another aluminum plate of the same size covered the top. A clip was used to clamp the plate together to form square sandwich. Sample holders of CN980, CN964, and CN964E75 were put in a 60 °C oven vertically for 48 hours. Those of CN980M50 were placed in the hood under room temperature. Each sandwiched sample of the oligomer stood vertically during the irradiation so that bubbles could rise to the top. These four series of urethane oligomers were irradiated with doses of 50, 100, 150, 200, and 250 kGy by the UMCP electron linear accelerator (LINAC) at 20.4 pulse/s and 15.6 Gy/pulse. Sample holders were arranged vertically and the distance between sample holders and the window of electron beam was 40 cm.

#### **3.3.2 Gamma Ray Irradiation**

Two different procedures were used for the sample preparation: one is the same as described in the above section; in another method, the oligomers were placed in a vacuum oven for 24 hours at 55 °C in order to remove the oxygen. The specimens were irradiated at 2 kGy/hr to doses of 50, 100, 150, 200, 250 kGy.

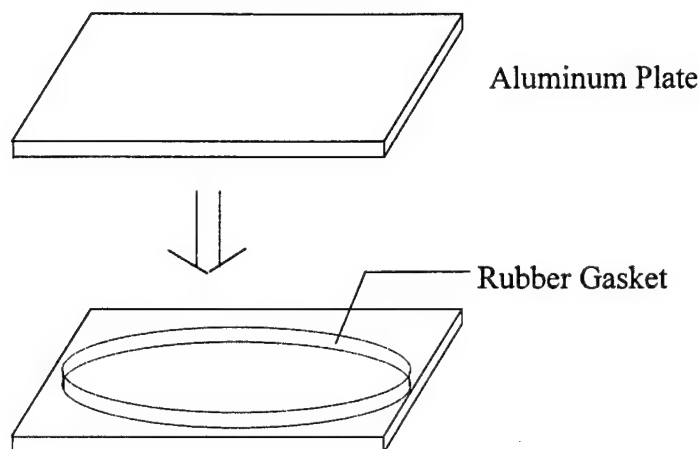


**Figure 5.** Sample holder for curing of urethane oligomers.

### 3.4 Grafting

Acrylonitrile was purified by distillation at vapor temperature 71 °C under nitrogen at the atmosphere pressure just before use. Polyurethane specimens were washed with n-hexane, dried under the hood for 24 hours then put in a vacuum desiccator for 24 hours just before use. The specimens were immersed in the acrylonitrile/n-hexane solution in a glass tube with nitrogen gas purging for 5 minutes before being sealed by a stopcock with a thin film of silicone vacuum grease on the glass joint; then the tube was put in the center of the gamma source where the absorbed dose rate was within 1 % of 210 Gy/min over two months in which these experiments were performed.

### 3.5 Gel Fraction

Gel fraction measurements were done by Soxhlet extraction. Three specimens of each cured product were prepared. Each specimen holder was cut into several small pieces. The specimen was placed in a porous thimble in the chamber with boiling toluene as the extracting solvent. Following the extraction, the thimble and gel were dried in a vacuum desiccator at 112 °C for 24 hours. After cooling to room temperature, the thimble and gel were weighted. Then the specimen was extracted again as described above. The extraction was terminated when constant weight after drying was achieved.

### 3.6 Hardness

Pacific Transducer Corporation's model 306L ASTM type A durometer was used to measure the hardness of cured products of CN980M50. Three pieces of a sample were stacked to a thickness of 9.5 mm, and placed on a hard, horizontal surface. The ancillary of the durometer was set below 5 points on the dial. The durometer was held vertically and the base was kept parallel to the surface of the specimen while the pressure foot was rapidly applied to the specimen. The minimum force required to obtain firm contact between the base and the specimen was applied. The maximum reading was obtained from after holding the durometer in place for 1-2 seconds. At least 5 tests were made on different positions to determine the average.

### **3.7 Low Energy Electron Bombardment**

Low energy electron bombardment was done by Dr. Sam Nablo at Electron Processing System (EPS) Inc. The dose rate was 50 kGy/pass.

### **3.8 Plasma Treatment**

Plasma surface treatment was done by Mr. Keith Neider of InPro Inc.

### **3.9 Mechanical Properties**

A Sintech Universal Machine (Sintech 20) was utilized to measure the mechanical properties. Tensile strength, elongation at break and modulus are obtained in accordance with ASTM D412, with a uniform rate of separation of 500 mm/min. At least three specimens with the same properties were tested.

## **CHAPTER 4**

### **RESULTS AND DISCUSSIONS**

#### **4.1 Abrasion Tests**

In this section, a standard test condition for measuring abrasion loss by means of the modified abrader described in **Section 3.2** will be discussed.

##### **4.1.1 Variables in Abrasion Test**

There are four main variables in the test conditions which affect the results: temperature, humidity, the applied load, and the nature of the abrasive paper. In this work, tests were performed at a fixed load under ambient temperature which might fluctuate slightly with time. Abrasion papers of silicon carbide (SiC) with three different grain sizes and aluminum oxide ( $\text{Al}_2\text{O}_3$ ) with one grain size were used in the survey. The types and specifications of those abrasive are listed in **Table 2**.

Grinding Materials	Grit No.	Hardness, $H_{abr}$ (MPa)	Grain Diameter ( $\mu\text{m}$ )
SiC	220	2,500	70
	400		30
	600		15
$\text{Al}_2\text{O}_3$	220	1,800	70

**\*Table 2.** Abrasive papers used and the corresponding values of hardness and grain size.

\* The information are provided by 3M Co.

Polyurethane absorbs moisture gradually and affects the energy dissipation during the abrasion test and, hence, causes fluctuation of the data. Therefore, the drying treatment described in the experimental part is necessary. Because of the limitations of the cutting tools (sharp knife), the width (length of contact with abrasive paper) of the specimens was not uniform. In order to eliminate this influence, the width ( $w_E$ ) was measured by a caliper and the abrasion loss data were normalized by a multiplying factor ( $1/w_E$ ). This approach is only valid when the difference between the width of the specimens is small. For instance, if the width is doubled, the abraded surface does not have the same shape. The reason is that the shape of both of the abrasive mounted on the drum and the folded specimens are arcs which were normal to each other (**Figure 6**). Experiments exhibited good agreement in the weight loss measurements when the length in contact with the abrasive paper was  $10 \pm 0.1$  mm. The main consideration for the use of 10 mm as the contact length was based on convenience. **Figures 7 and 8** show the abrasion loss for PU composites rubbing

against different abrasive papers. Harder grinding material and/or larger grain size caused larger abrasion loss. It should be noted that all of the abrasive papers have sharp asperities; therefore, the wear mechanism was dominated by abrasive wear. For No. 400 and 600 SiC abrasive papers, the rate of abrasion loss tended to decrease at higher cycles. On the other hand, against No. 220 SiC and  $\text{Al}_2\text{O}_3$  abrasive papers, the specimens showed an almost linear relationship between abrasion loss and number of abrasion cycles. Since the specimens were repeatedly abraded on the same track, the accumulation of the debris protected the part of the specimens from being worn by the abrasive grains. Such an effect is not significant in the case of large grain sizes, because the voids between the grains are larger and most of the grains are not covered by the debris. It should be also noted that the abrasion area changes during the measurement (**Figure 8**). This makes it hard to establish a useful quantitative equation to describe the abrasion loss. However, the measurements provide a useful comparison of relative resistance to edge abrasion.

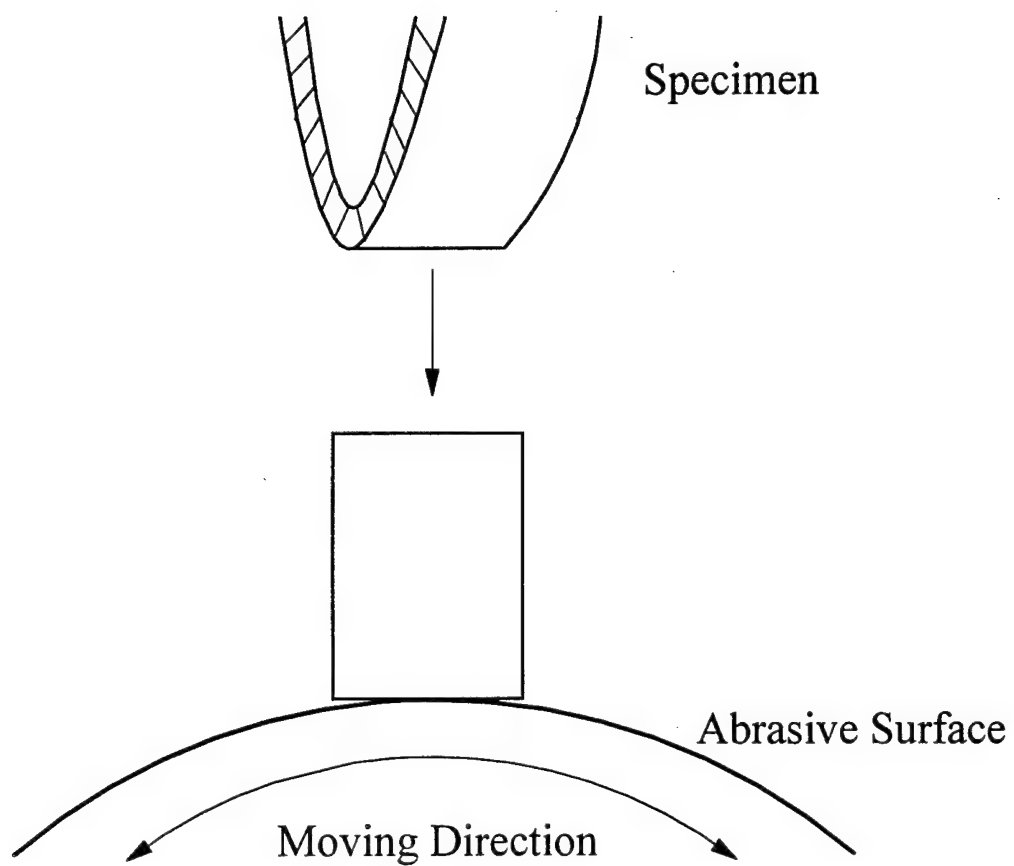


**Figure 6.** Geometry of abrasive and abraded surfaces.



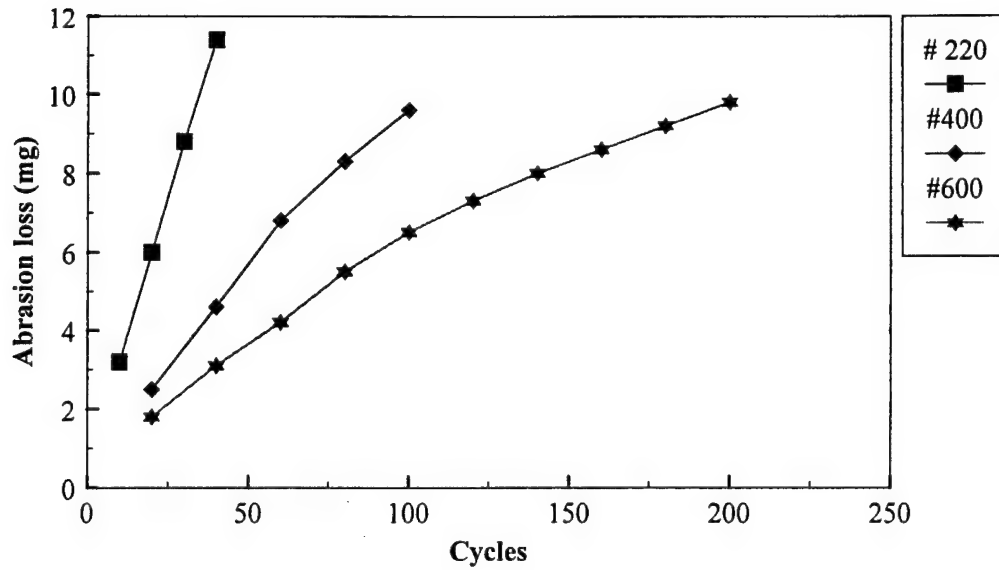


Figure 7. Abrasion loss vs. cycles for the PU sliding against SiC abrasive papers with different grain sizes.

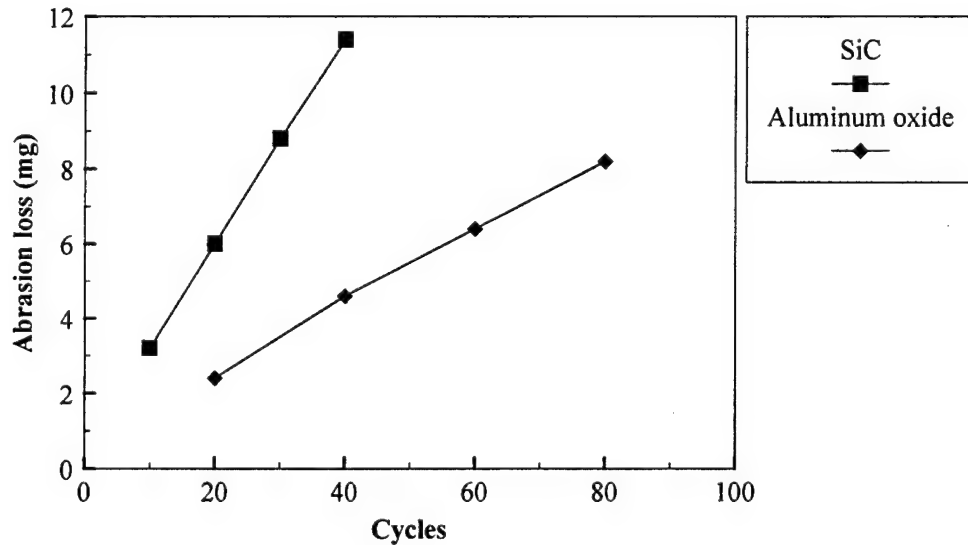
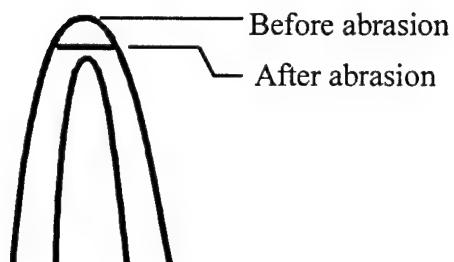


Figure 8. Abrasion loss vs. cycles for the PU sliding against abrasive papers with the same grain size but different grinding materials.



Shape before clamped  
to the paper clip



Shape while mounted  
in apparatus



Shape after released  
from apparatus

**Figure 9.** The shape of the specimen at different times.

#### **4.1.2 Abrasion Loss in Different Sides**

The polyurethane sheets had a shiny smooth side and a side that was dull and apparently rough. The sheets were slightly curved, with smoother surface as the outside surface and the "rougher" surface on the inside. Stresses needed for bending specimens with different sides as abraded surface were different. The smoother side was suggested by the supplier as the surface for abrasion measurements and treatments. However, no difference in abrasion loss was observed for abrading the two sides.

## 4.2 Polyurethane from irradiation curing

New polyurethane materials which were tested as possible replacements of the materials currently in use were synthesized here by curing urethane acrylate oligomers by ionizing radiation. Characterization and abrasion resistance of these materials are shown in below.

### 4.2.1 Gel Fraction

Electron beam (EB) irradiation was used in the first attempt to cure the acrylate urethane oligomers. The results of Soxhlet extraction shows the gel fraction reaches maximum at the dose of 150 kGy (**Figure 10**). Several factors which contribute to this behavior, the principal ones being the result of rapid heating at higher dose rate (up to 65 cal/g) by the electron beam and at least as much from the heat of polymerization. Among the four different series of oligomers, only the products of CN980M50 were resilient, and the hardness of its products does not decrease with the decrease in gel fraction when the dose exceeds 150 kGy (**Figure 11**). Therefore, a reaction condition with better temperature control was necessary. Another set of radiation curing experiments were performed by gamma ray irradiation for CN980M50 with and without de-oxygenation. The gel fraction data are shown in **Figure 12**. They show that oxygen inhibits the curing. The relationship between dose and hardness of the cured de-oxygenation oligomer is shown in **Figure 13**. The much lower dose rate associated with the gamma irradiation caused relatively low temperature rise and an expected pattern to the data.

#### 4.2.2 Abrasion Loss

The debris of the specimen stuck to the abrasive counterparts and made the latter totally smooth after 100 cycles. No. 600 SiC abrasive papers were used in the measurements because the wearing of the specimens by No. 220 SiC papers were too fast to yield a difference between different materials for abrasion resistance. Only the products cured by gamma ray irradiation were investigated. **Figure 14** and **15** show the abrasion loss and abrasion loss rate at different cycles. Since the fact that the debris in this case formed protective layers on the abrasive counterparts (this could be easily observed from the quickly decrease in the abrasion loss rate), only the data after 20 cycles was taken into account. By this procedure, the material with higher gel fraction had a better abrasion resistance.

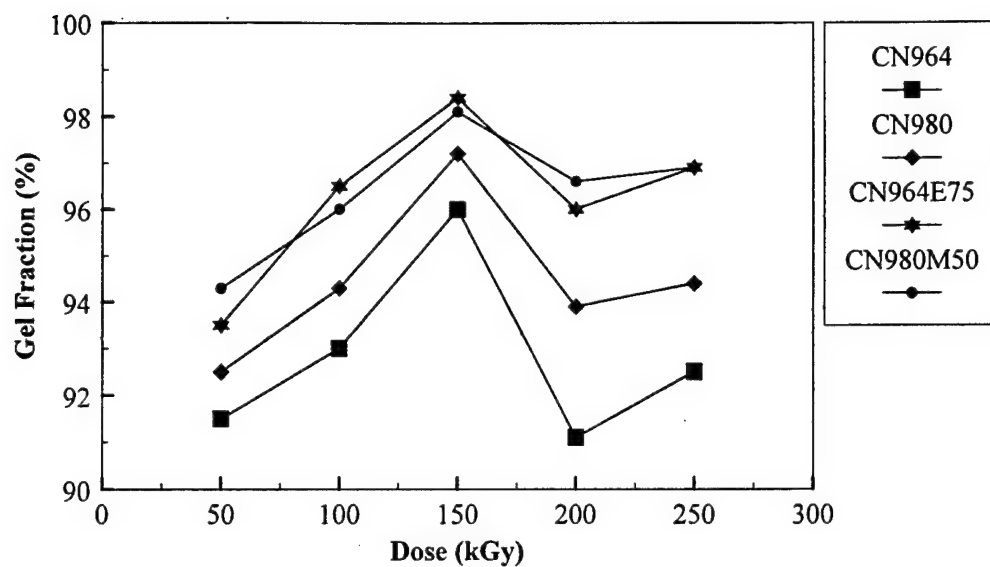


Figure 10. Gel fraction vs. doses for EB cured urethane oligomers.

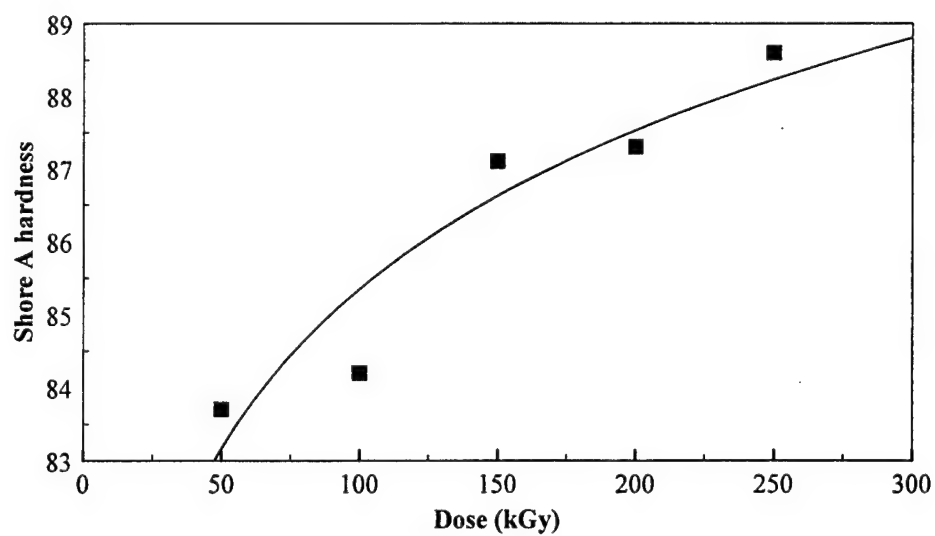


Figure 11. Shore A hardness of cured CN980M50 at different EB doses.

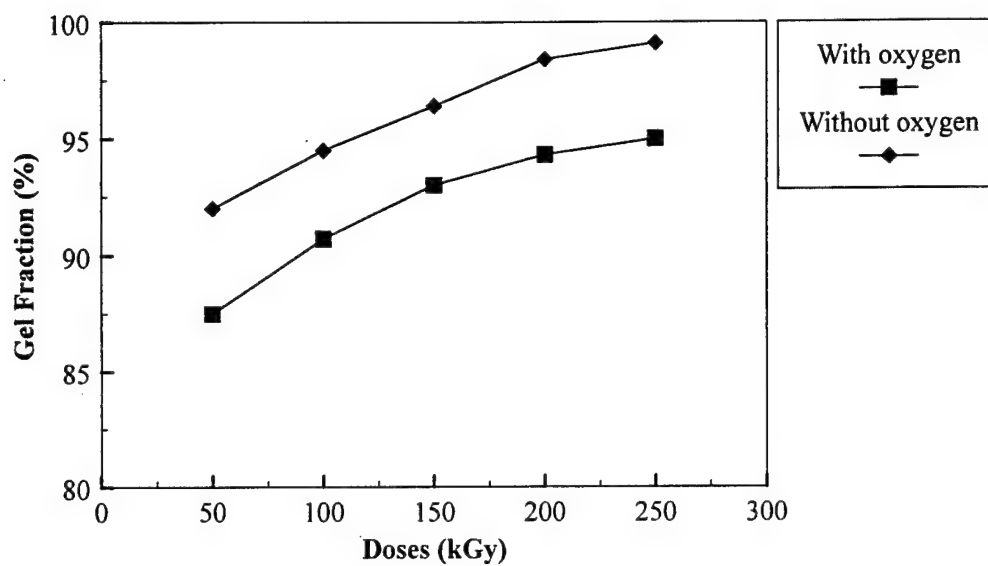


Figure 12. Gel fraction vs. doses for CN980M50 cured by gamma ray irradiation

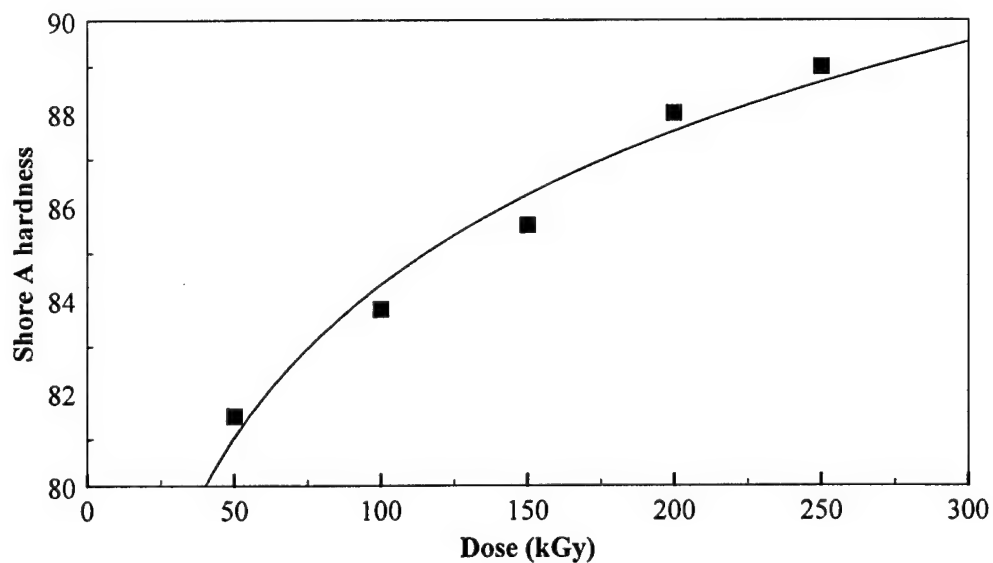


Figure 13. Shore A hardness of CN980M50 cured by gamma ray irradiation

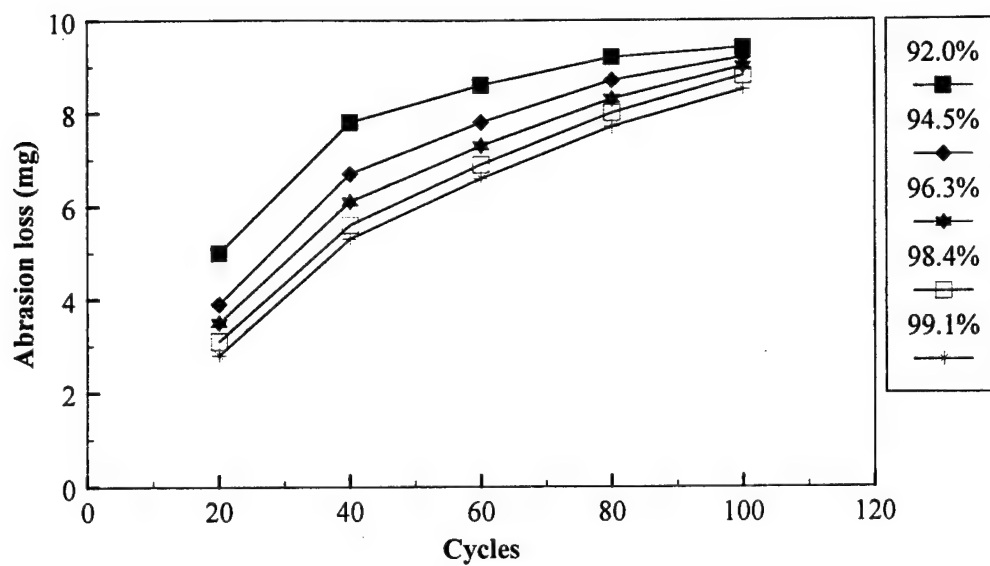


Figure 14. Abrasion loss vs. cycles for cured CN980M50 with different gel fractions.

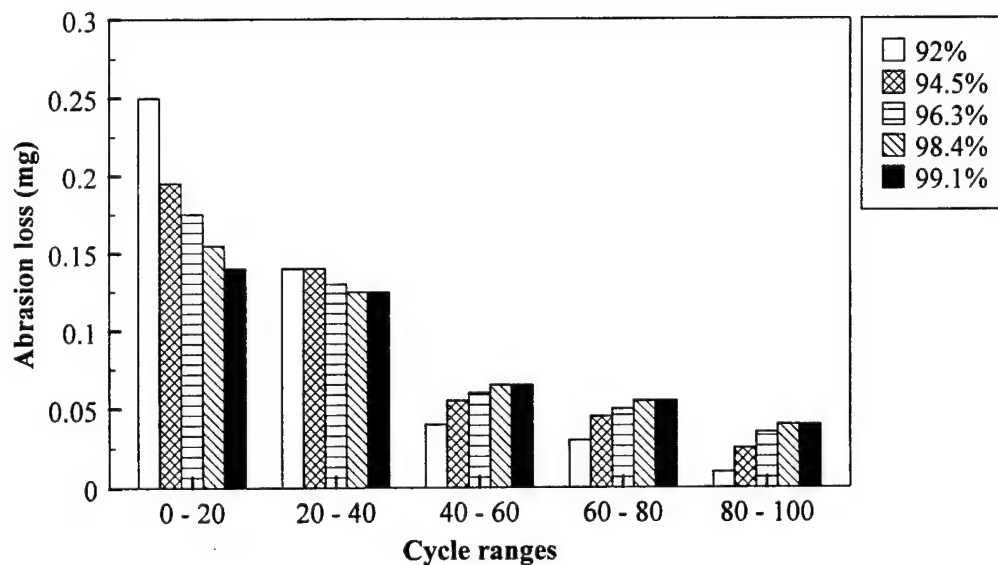


Figure 15. Abrasion loss rates for cured CN980M50 with different gel fraction at different cycle ranges.



### 4.2.3 Hardness and Abrasion Loss

**Figure 16** shows an almost linear relationship between Shore A hardness and gel fraction. **Figure 17** shows that abrasion loss decreases as the hardness increases. This is in agreement with the work of Buist and Davies [53] (**Equation 5**), and with the behavior of rigid polymers (see **Chapter 2**). However, it conflicts with the relation proposed by Li and Hutching [71] who suggest that the erosion rate increases as the hardness of polyurethane increases. In their case, the erosion takes place while blowing abrasive particles (e.g. silicone carbide) over the specimens. A softer specimen finds it easier to recover from the deformation caused by the attacking particles than the rigid one without being cut. In our investigation, a normal load was applied on the specimen when it rubbed against the abrasive counterface. The specimen surface was plowed and cut. In this case, the harder material has higher crosslink density (gel fraction) which means the binding strength between molecules is higher and the abrasion resistance is greater. Sofuku [72] observed that abrasion loss first decreases as the hardness increases then increases beyond a certain hardness. He used polyurethanes with the same hard segment but with different soft segment chain lengths, however, in our study, the compositions of materials are the same. Friedrich [60] proposed that, for specimens rubbing against abrasive papers, abrasion loss is caused by plowing, microcracking, or both. The magnitude of these effects are determined by the applied pressure,  $p$ , and the critical pressure of the specimen,  $p_{crit}$  (which is proportional to fracture toughness/hardness). When  $p < p_{crit}$ , plowing effects dominate and less abrasion loss is registered with samples of higher hardness.

Microcracking dominates where  $p > p_{crit}$  in which case, higher hardness causes larger abrasion loss (**Equation 3**).

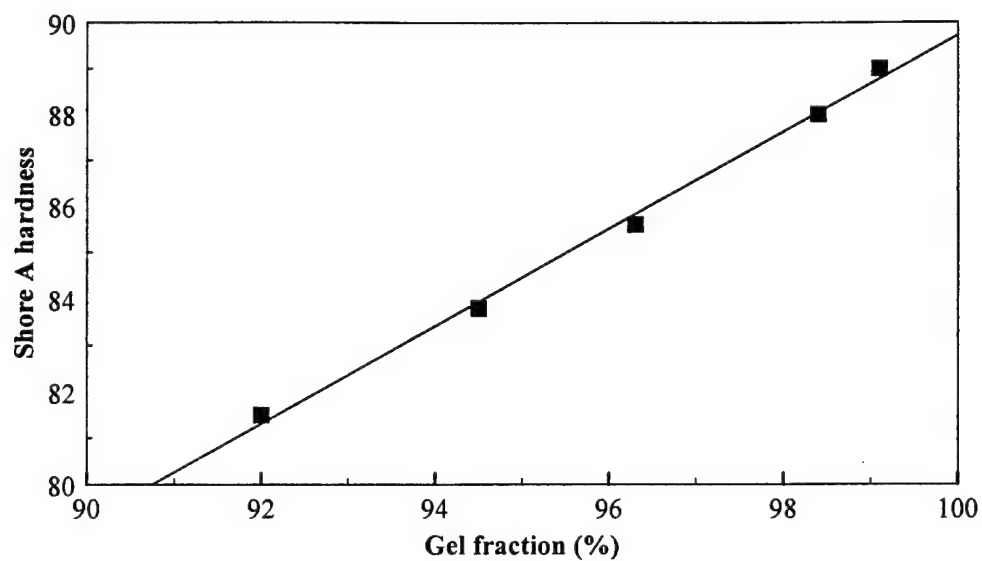


Figure 16. The relation between shore A hardness and gel fraction for the cured CN980M50.

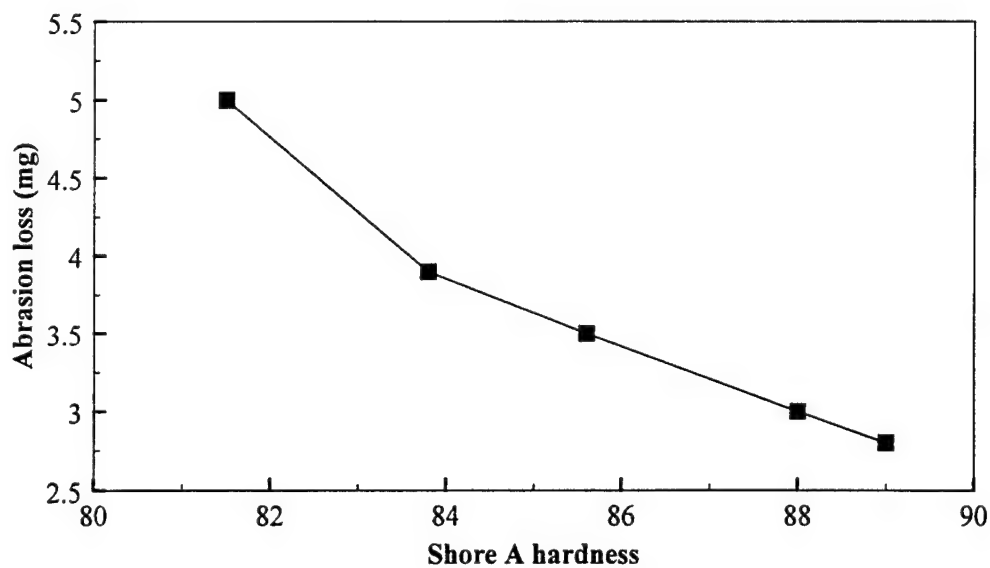


Figure 17. Abrasion loss vs. hardness for the cured CN980M50 after 20 cycles.

### 4.3 Surface Treatment by Low Energy Electron Beam

Abrasion resistance of the new polyurethane materials polymerized in this work and discussed in **Section 4.2** is worse than the one provided by Ft. Belvoir and which is currently in use. Also, from **Section 4.2**, polyurethane with higher crosslink density shows greater abrasion resistance. Therefore, low electron energy treatment was attempted on the surface of polyurethane composites currently in use.

The penetration depth of electrons is related to their energy. For plane parallel beams incident normally on a slab absorber, the useful penetration is given by the following:

$$x \text{ (cm)} \approx \frac{E^2}{\rho}, \text{ when } E < 1 \text{ MeV},$$

$$x \text{ (cm)} \approx \frac{E}{\rho}, \text{ when } E \geq 1 \text{ MeV},$$

where  $x$  is the penetration depth,  $E$  is the energy of electron, and  $\rho$  is the density of material ( $\text{g/cm}^3$ ). In this study, some irradiations were done with electrons with energy 175 keV with a dose rate of 50 kGy/pass; the useful penetration was a few microns. The abrasion loss of PU materials thus irradiated is shown in **Figure 18**. It shows there is no significant improvement for the materials after treatments up to 200 kGy. This approach was abandoned in favor of the graft polymerization method of modifying the surface (**Section 4.5**), especially as it was difficult to arrange for access to EPS Inc. accelerator in Massachusetts.

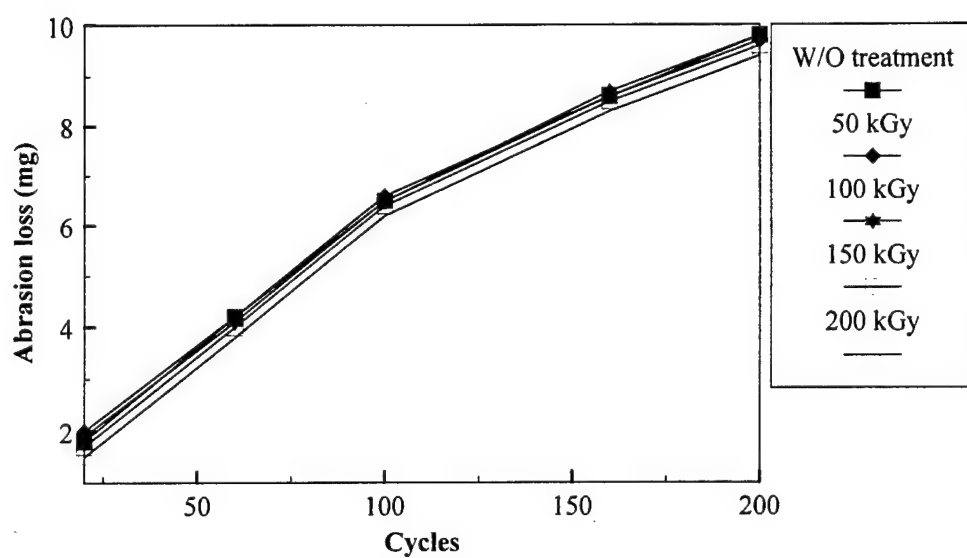


**Figure 18.** Abrasion loss of PU with low energy EB treatment.

## 4.4 Surface Treatment by Plasma

Plasma treatments also can be used to harden material surfaces. There were three different plasma treatments used in this investigation: (1) propane treatment followed by a fluorine treatment, (2) fluorine treatment only, (3) oxidation treatment only. **Figure 19** shows there is no improvement in abrasion resistance after these treatments. This was a limited exploratory effort which was not considered for further work, not only because of lack of early success, but because of the more promising results obtained by graft polymerization (**Section 4.5**).

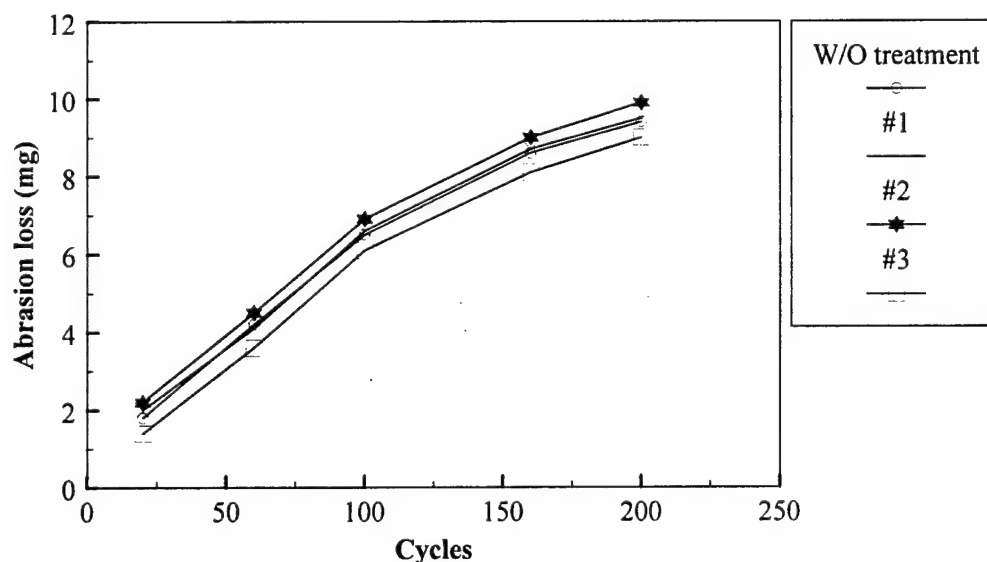


**Figure 19.** Abrasion loss of plasma-treated PU.

## 4.5 Polyacrylonitrile Grafted Polyurethane (PAN-g-PU)

Since methods discussed in Section 4.2, 4.3, and 4.4 did not provide improvement in abrasion resistance. Another approach was taken to improve abrasion resistance by grafting a vinyl monomer to the polyurethane backbone. Acrylonitrile as the monomer was chosen because of the attractive properties of polyacrylonitrile. It is a semi-crystalline glassy material ( $T_g = 105^\circ\text{C}$ ) with (1) good chemical resistance, (2) high abrasion resistance, and (3) good mechanical properties. Polyacrylonitrile can be used to form thin layer on the surface of elastomers with minimal change in bulk mechanical properties of elastomers.

### 4.5.1 Nature of Graft

The term "graft polymerization" is often loosely applied to a reaction whereby a polymer undergoes a weight gain consisting of (1) a true chemically bonded fraction of pendant chains and (2) occluded homopolymer which is alloyed with or heterogeneously dispersed in the matrix. Also, the weight gain can be uniform or distributed in a non-uniform manner determined by diffusion and solubility properties during grafting. In order to determine the nature of graft a solvent experiment was performed. Small pieces of grafted and ungrafted polyurethanes were immersed in tetrahydrofuran (THF). The ungrafted one, which was irradiated in pure n-hexane by a 20 kGy gamma dose, dissolved quickly, and the inert fillers inside made the solution turbid. The grafted polyurethane in THF made the solution only slightly turbid and the polymer showed a sandwich-like structure; it appeared to consist of insoluble PAN-grafted surfaces containing a relatively clear ungrafted interior. After prolonged

immersion in THF, the sandwich separated into two curled sheets with the outer surface inside. If there were only polyacrylonitrile generated in the polyurethane matrix, the specimen would dissolve completely and polyacrylonitrile particles would disperse in the solution. In order to make sure the phenomenon is caused by the polyacrylonitrile graft, an ungrafted polyurethane was sliced to half thickness and immersed in benzene and the flat sheets did not curl. The above observations confirmed that the grafting produced a true graft with little homopolymer and the grafting is heavier on the surface than inside of the polyurethane (**Figure 20**). In order to examine if crosslinking occurred, grafted samples were soaked in N,N-dimethylformamide (DMF). DMF is a good solvent for both polyurethane and polyacrylonitrile. Experiments showed all specimens dissolved completely. This result indicates that no crosslinking occurs in the matrix.

#### **4.5.2 Graft Yield**

In order to preferentially graft polyacrylonitrile to the surface of the polyurethane, n-hexane was chosen as the solvent. The data from the swelling tests shows polyurethane swells n-hexane much more slowly than the other organic solvents studied (cyclohexane, chloroform, methanol, ethyl acetate, and benzene). Of course, uniformity of swelling is time dependent and the extent of swelling is concentration dependent. Experiment showing the swelling of polyurethane in AN/n-hexane solutions produced the data given in **Figure 21**. **Table 3** shows the graft conditions and yields of polyacrylonitrile grafted polyurethane (PAN-g-PU).



In order to investigate the inhibition of grafting by oxygen, several specimens were exposed to air in a dry-seal desiccator for two weeks before irradiation. Specimens with and without exposure to air were placed in the same container and irradiated. **Table 4** lists the grafting conditions and **Figure 22** shows that oxygen inhibition of grafting is reduced at higher dose.

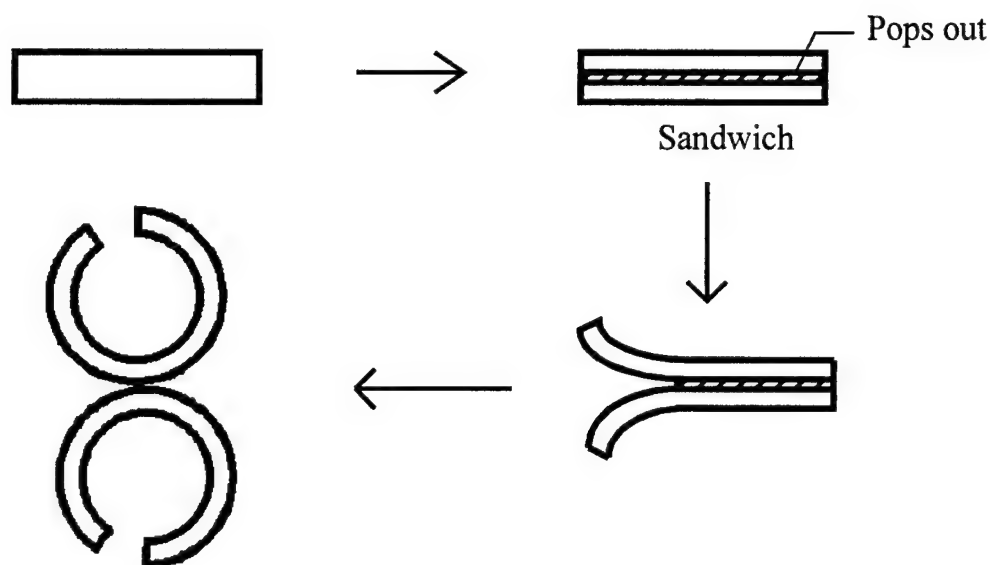


**Figure 20.** PAN-g-PU in THF.

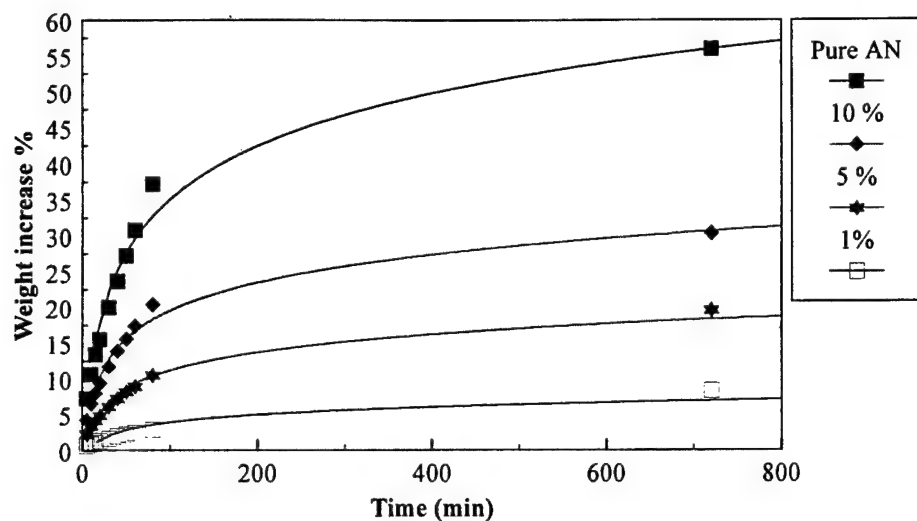


Figure 21. The swelling of PU (wt. %) in different concentration of AN/n-hexane solution (vol. %).

Vol. % of acrylonitrile in the solution	Swelling Time before Irradiation (min.)	Dose (kGy)	Dose Rate (Gy/min)	Irradiation Time (min.)	Graft Yield (%)
10	40	20	212	94.3	20.2
10	40	20	211	94.6	20.7
10	20	10	212	47.2	13.8
10	20	10	211	47.3	13.4
10	10	10	209	47.9	10.4
10	10	8	210	38.1	8.6
10	10	5	212	23.6	5.8
10	10	5	211	23.7	5.9
10	10	2	212	9.4	1.5
10	10	2	211	9.5	1.5
5	10	14.7	211	70	4.9
1	10	25.2	210	120	1.4

Table 3. The graft conditions and yields of PAN-g-PU

Swelling Time before Irradiation (min)	Dose (kGy)	Dose Rate (Gy/min)	Irradiation Time (min.)	Graft	Yield (%)
				With O <sub>2</sub>	Without O <sub>2</sub>
10	1	210	4.8	0	0.5
10	2	210	9.5	0.2	1.5
10	5	210	23.9	4.9	5.9
10	10	210	47.7	9.5	10.3
10	20	210	95.4	12.4	12.8

**Table 4.** Graft conditions and yields of PAN-g-PU in the 10% AN/n-hexane solution.

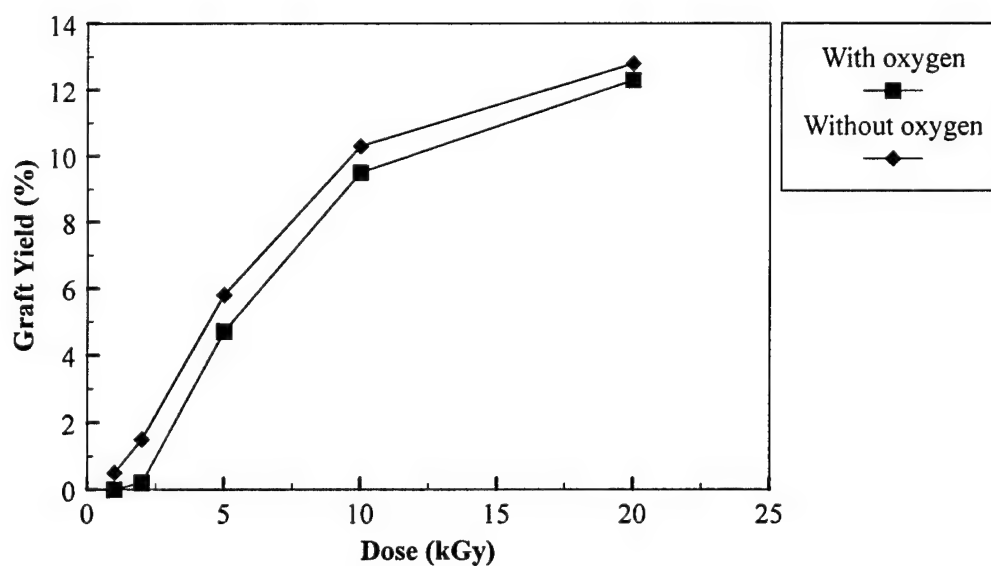


**Figure 22.** The Relation between graft yields and doses for PAN-g-PU.

The dose and acrylonitrile permeation into the polyurethane are the two main factors affecting the graft yield. Comparison of **Table 4** to **Table 3** shows that at doses of 10 and 20 kGy, the graft yields depend on the amount of acrylonitrile in the polyurethanes. In **Figure 22**, the curve tends to level off quickly at higher doses because the irradiation also produces polyacrylonitrile homopolymer in the solution and, hence, reduces the concentration of acrylonitrile available for grafting. The dependence of graft yields on the dosage at low doses can be seen in **Table 5**. The yields are less than the acrylonitrile concentration before irradiation. The graft yield in **Table 3** is proportional to  $D^{1.5}$  up to  $D = 5$  kGy. Such an empirical fit has no fundamental meaning because it combines the changes with dose in monomer concentration in the solution, which, in turn, controls monomer concentration in the polymer. This is shown in **Table 6** where monomer concentration alone (not graft yield) determines swelling characteristics.

Pre-swelling time (min.)	Wt. increase after pre-swelling (%)	Dose (kGy)	Total swelling time (min.)	Estimated weight increase (%)	Graft Yield (%)
40	13.9	20	134	> 23	20.2
10	6.5	20	105	> 20	12.8
20	11.8	10	67.2	> 17	13.8
10	6.5	10	57.7	> 16	10.3
10	6.5	8	48.1	> 14	8.6
10	6.5	5	33.7	> 12	5.9
10	6.5	2	19.4	> 8	1.5
10	6.5	1	14.8	> 6	0.5

**Table 5.** The comparison of acrylonitrile intake and graft yield.

Graft Yield (%)	AN vol. % in AN/ n-hexane	Weight increase % after			
		60 min.	120 min.	180 min.	48 hr
20.2	0	0.6	0.9	1.2	5.1
20.2	10	16.6	25	27.7	29.9
20.2	100	30.1	47.9	54	55.8
13.8	0	0.8	1.2	1.5	5.6
13.8	10	16.8	25.3	28	30
13.8	100	31	47.7	54	56.3
5.9	0	1.4	2	2.5	6.6
5.9	10	17	25.2	28	29.7
5.9	100	30.8	48	53.3	55.5
1.5	0	1.5	2.2	2.7	7.2
1.5	10	17.5	25.5	28.4	30.5
1.5	100	31.1	48	54	56
0	0	1.7	2.5	3.1	7.4
0	10	17.4	25.7	28.6	30.3
0	100	30.8	47.5	53.7	56

**Table 6.** The swelling data of PAN-g-PU.

Although the swelling of acrylonitrile is independent of graft, **Table 6** shows that the grafting of polyacrylonitrile onto polyurethane inhibits the swelling by n-hexane. This is a further evidence for that the leveling-off of the graft yields at the higher doses is caused by the homopolymerization of acrylonitrile in the outside solution. **Table 6** and **7** show that the swelling is concentration dependent; **Table 7** also shows the dependence on solvent. The lower solubility and diffusivity of water in polyurethane cause a lower swelling ratio of the acrylonitrile aqueous solution. Lokhande et. al. [77] grafted acrylonitrile onto guar gum by immersing the gum in acrylonitrile aqueous solution and then submitting the swollen sample to gamma radiation. They found the graft yields increased with the increase of acrylonitrile concentration in the solution while other conditions were kept the same.

Solution	Weight	increase %	after
	60 min	120 min	48 hr
10% AN/ n-hexane	17.4	25.7	30.3
5% AN/ n-hexane	8.9	12.5	19.6
1% AN/ n-hexane	2.5	3.5	8.7
Pure n-hexane	1.7	2.5	7.4
5 % AN/ water	3.4	4.7	8.9
1% AN/ water	0.9	1.1	2.1
Pure water	0.6	0.7	1.3

**Table 7.** The swelling of polyurethane in the different solution systems.

### 4.5.3 Abrasion Loss

**Figure 23** shows the abrasion scheme of a grafted PAN-g-PU sample which is shown in a simplified 3-region form. The two surfaces may have different graft content and the core of the sample is virtually ungrafted. Such a one-sided surface graft is intended to provide improved abrasion resistance to the surface in normal use with little change in bulk mechanical properties. In the beginning of the edge abrasion test, only the harder (or more heavily grafted) zone was abraded. After the wearing out of the crest, the softer and harder zones were in simultaneous contact with the abrasive paper. Visual observations show that the size of the debris from the grafted polyurethanes, especially for graft yields larger than 5.9 %, were smaller than the ungrafted ones at the beginning of abrasion. With 5.9 % graft significantly larger debris appear after 100 cycles. The size difference of debris between 1.5 % grafted and ungrafted polyurethane could not be distinguished by the naked eye. According to the equation of Mitsuhashi [64] (**Equation 15**), the larger debris size indicates a larger abrasion loss. **Figure 24** compares the abrasion loss for PAN-g-PU synthesized from 10 % AN/ n-hexane solution with result from different grafts. The abrasion loss seems to level-off for 13.6 % and 20.5% grafted PAN-g-PU. However, **Figure 25** shows that the abrasion loss rates in the first 60 cycles are almost identical for both of them, and for a larger cycle number, that the 13.6 % graft lost its weight faster than the 20.5 % graft. This may indicate that both have similar surface graft densities (PAN weight/unit weight of surface) but the depth of the graft is different. In **Figure 25**, the abrasion loss rate decreases with increasing cycle number for 0 % and 1.5 % grafted

polyurethanes; this is probably due to the protection by the debris. On the other hand, for other PAN-g-PU, the abrasion loss rate increases in the cycle range of 60 - 100. This is the effect of change in the graft density in overcoming the effect of debris protection; and after 100 cycles, debris protection becomes stronger.

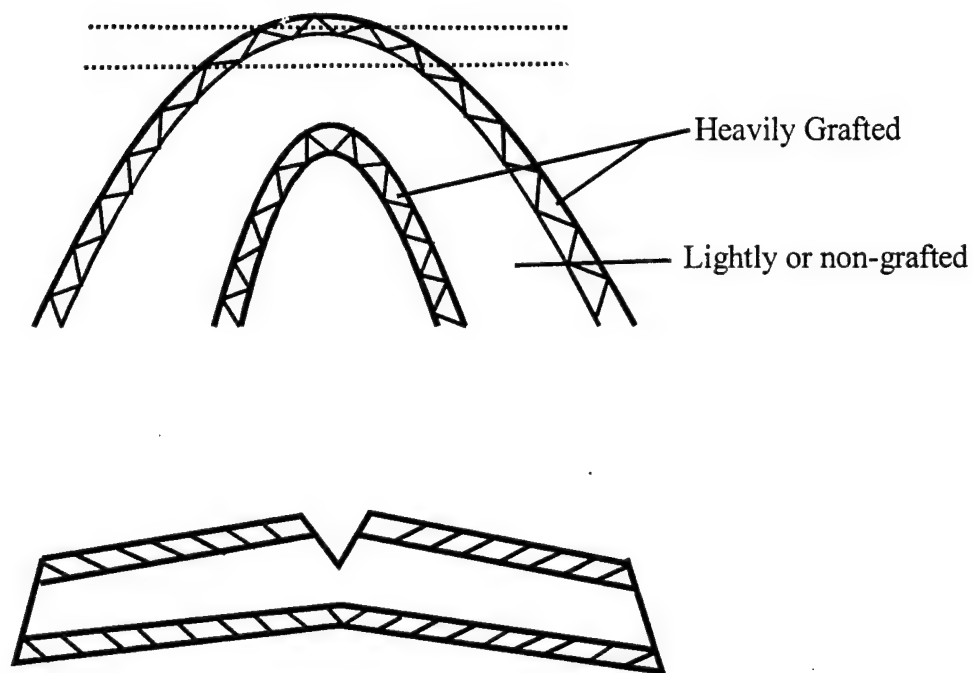


**Figure 23.** The abrasion scheme of PAN-g-PU.



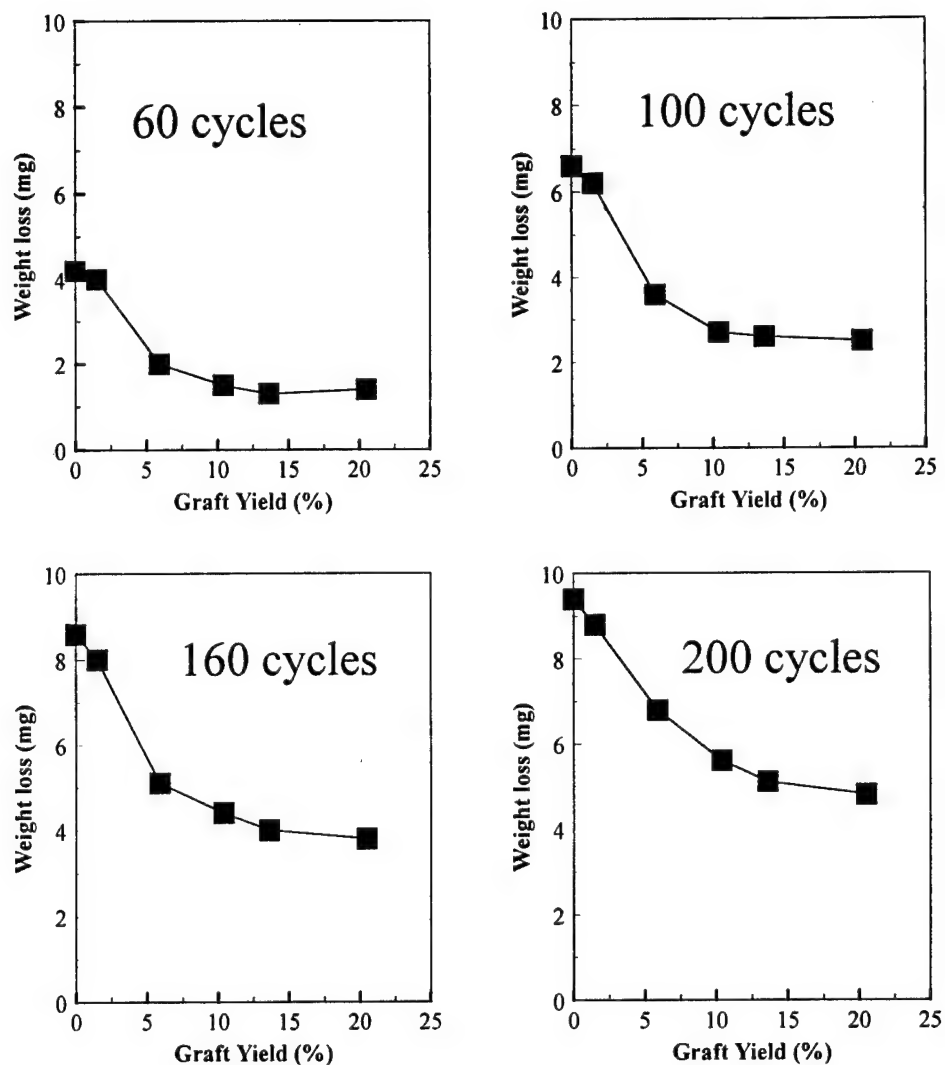
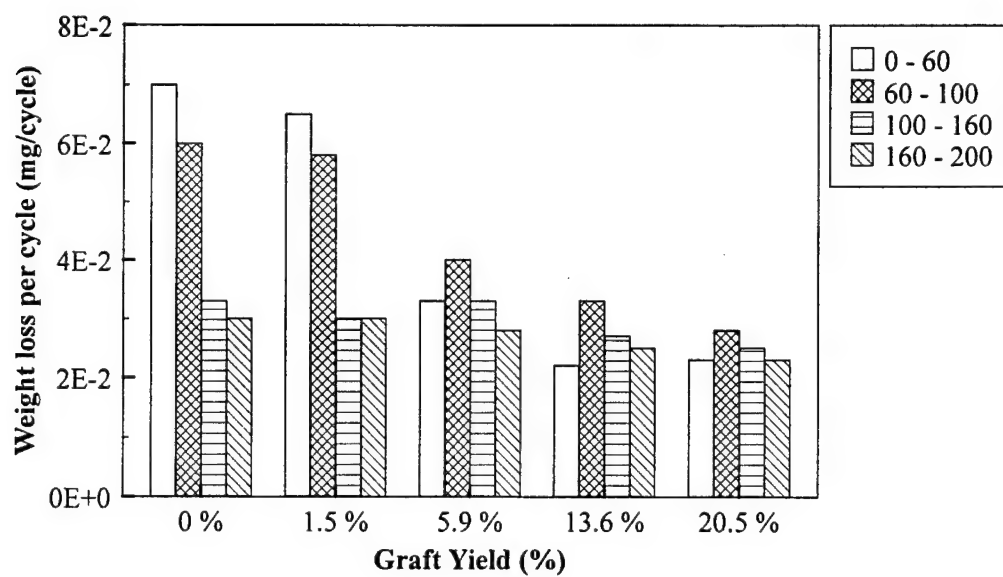


Figure 24. Abrasion loss of PAN-g-PU synthesized from 10% AN/n-hexane with different graft yields.



**Figure 25.** Abrasion loss rate of PAN-g-PU.

#### 4.5.4 Heat Treatment

Polyacrylonitrile has been found to crosslink upon heating (**Figure 26**) [79, 80]. An azomethine ((1), **Figure 26**) is formed by heating at 80 °C. Heating at a higher temperature (135 °C) produces the conjugated fused ring of the polyimide ((2), **Figure 26**).

PAN-g-PU and ungrafted polyurethane were put into a vacuum desiccator at 80 °C for 24 hours. After this treatment, the PAN-g-PU with 13.6 % and 20.5 % graft were stiffer than before the heating but no appreciable color change was observed. Part of the materials were cut and heated at 135 °C under vacuum for 20 hours. Only 13.6 % and 20.5 % grafted polyurethanes showed significant changes in color by turning to reddish yellow; however, the stiffness decreased. **Table 8** lists the change in abrasion loss for PAN-g-PU after heat treatments. It can be seen that only 13.6 % and 20.5 % grafts after 80 °C treatment give rise to substantial improvements in abrasion resistance. However, further heating at 135 °C reduces abrasion resistance.

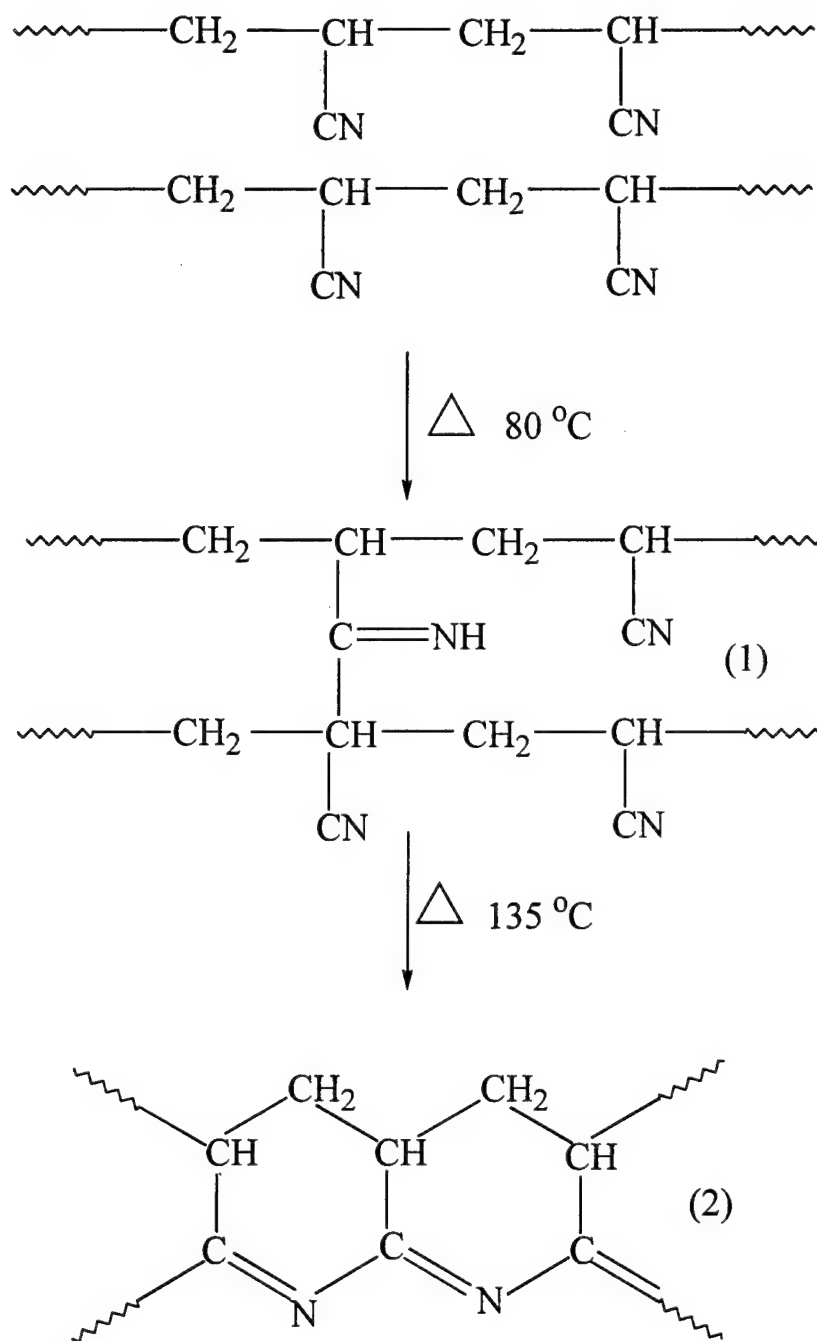


**Figure 26.** Crosslinking of Polyacrylonitrile.

**Graft % = 20.5**

	Weight loss (mg)		
Cycles	Without heat treatment	@ 80 °C 24 hr	@80 °C 24 hr & 135 °C 20 hr
100	2.5 ± 0.2	1.7 ± 0.3	2.5 ± 0.3
200	4.9 ± 0.3	4.0 ± 0.2	4.9 ± 0.2

**Graft % = 13.6 %**

	Weight loss (mg)		
Cycles	Without heat treatment	@ 80 °C 24 hr	@80 °C 24 hr & 135 °C 20 hr
100	2.6 ± 0.3	2.0 ± 0.2	2.5 ± 0.3
200	5.2 ± 0.2	4.5 ± 0.2	5.1 ± 0.3

**Graft % = 5.9 %**

	Weight loss (mg)		
Cycles	Without heat treatment	@ 80 °C 24 hr	@80 °C 24 hr & 135 °C 20 hr
100	3.3 ± 0.2	3.1 ± 0.3	3.3 ± 0.3
200	6.7 ± 0.3	6.8 ± 0.3	6.8 ± 0.3

**Graft % = 1.5 %**

	Weight loss (mg)		
Cycles	Without heat treatment	@ 80 °C 24 hr	@80 °C 24 hr & 135 °C 20 hr
100	6.2 ± 0.3	6.3 ± 0.3	6.3 ± 0.3
200	9.2 ± 0.4	9.1 ± 0.4	9.2 ± 0.4

**Table 8.** The comparison of abrasion loss for PAN-g-PU before and after heat treatment.

### 4.5.5 Grafting and Changing Bulk Properties

Figure 24 shows that grafted polyurethanes have almost a factor of two advantage in abrasion resistance over untreated polyurethane. Furthermore, post-grafting heat treatment at 80 °C improves the abrasion resistance by more than a factor of two (Table 8). However, the accompanying increase in stiffness of the elastomer is not acceptable. Efforts to remain flexibility while improving abrasion resistance are necessary. This led to the attempt to restrict the graft only to the surface of polyurethane.

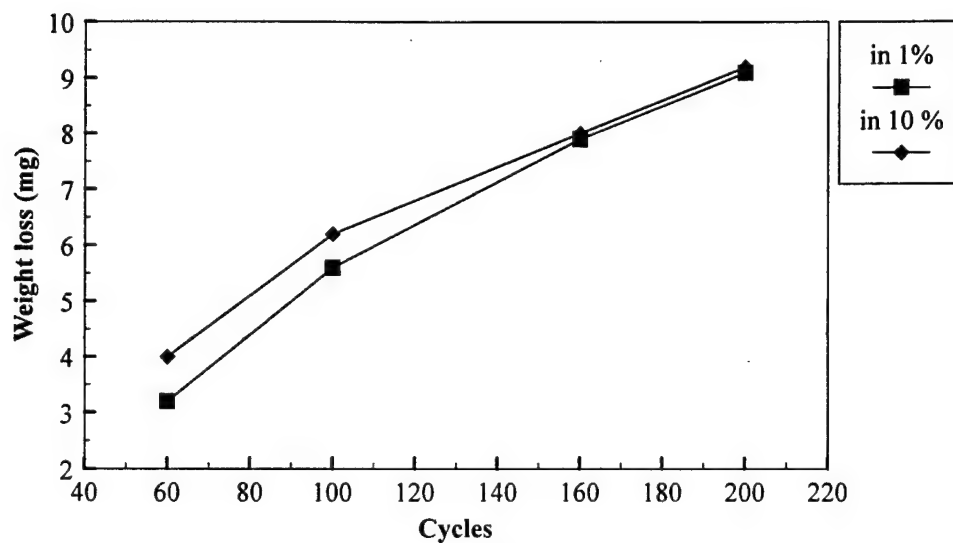
#### 4.5.5.1 Surface Grafting

Since polyurethane swells with acrylonitrile rapidly (see Figure 21), the graft density of polyacrylonitrile is high in the bulk polymer, which changes the bulk properties of the elastomeric polyurethane matrix and makes it stiffer. Thus, efforts were made to constrain the grafting to the surface. According Figure 21 and Table 7, polyurethane swells much more slowly in 1 % AN/n-hexane solution. Also, the graft of acrylonitrile on the polyurethane does not affect the acrylonitrile intake (Table 6). A graft experiment was performed to make the polyurethane specimen described in Table 9.

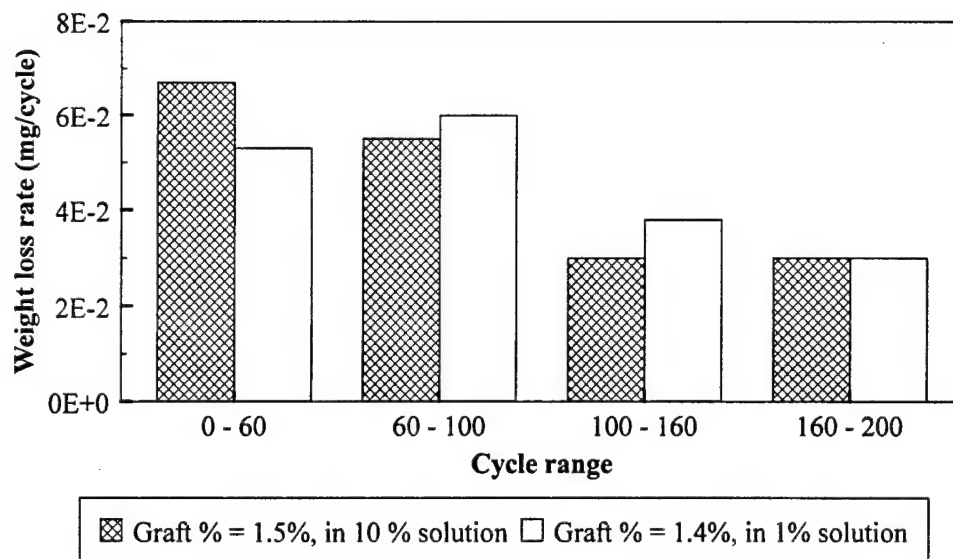
Pre-swelling time in 1 % AN/n-hexane (min.)	Dose (kGy)	Dose rate (kGy/min)	Irradiation time (min.)	Graft %
10	25.2	209.9	120	1.4

Table 9. Graft condition.

The graft yield, 1.4 % was low because most of acrylonitrile polymerized in the external solution before diffusing into the polyurethane. Comparing this PAN-g-PU to the one with similar graft yield (1.5 %) synthesized from 10 % AN/n-hexane solution, the abrasion loss data of the former had better abrasion resistance in the first 60 cycles, but both had similar abrasion loss after 200 cycles (**Figures 27 and 28**). This indicates the PAN-g-PU synthesized from 1 % AN/n-hexane had a larger graft density on the surface. However, graft yield was not enough to improve the abrasion resistance significantly.



**Figure 27.** The comparison of abrasion loss for PAN-g-PU with similar overall graft yield but synthesized from different monomer concentrations.



**Figure 28.** The abrasion loss rate for PAN-g-PU with similar overall graft yield but synthesized from different monomer concentrations.



#### 4.5.5.2 Choice of Grafting Conditions

The swelling and grafting results summarized in **Figure 21** and **Table 3** led to the choice of 10 % AN/n-hexane solution as the optimum means of obtaining high enough graft (> 10 %) to improve abrasion resistance substantially (**Figure 24**), and concentrated near the surface (10 min pre-irradiation equilibration). The stiffness increase problem was addressed by the one-side grafting method described in the next section.

#### 4.5.5.3 Graft on One Side

Attempts to restrict grafting to one side were performed by covering the other side with Scotch Magic Tape. **Table 10** shows the reaction conditions and graft yields of PAN-g-PU synthesized from 10 % AN/n-hexane solution with 10 minutes equilibration time. Pieces of grafted materials were immersed in THF. There was a thin layer of insoluble material remaining on the side with tape attached; this indicates the tape could not totally inhibit the penetration of acrylonitrile into polyurethane. However, this layer was much thinner than the insoluble layer on the exposed side. The abrasion loss data are for the exposed shown in **Figure 29**.

Dose (kGy)	Graft Yield (%)
8	4.1
10	5.1
20	6.8

**Table 10.** Graft yields of one side grafted PAN-g-PU.

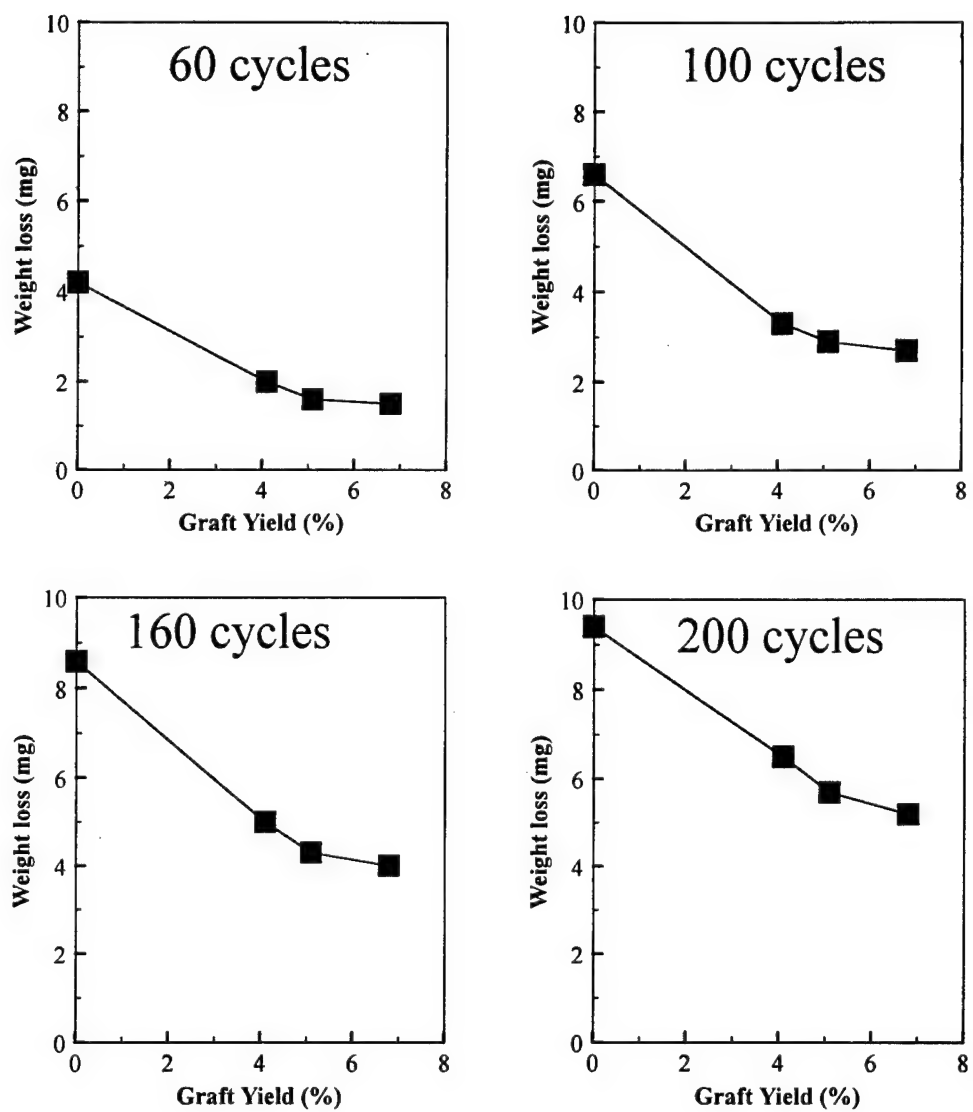


Figure 29. Abrasion loss vs. graft yield for one side grafted PAN-g-PU.

#### 4.5.5.4 Mechanical Properties

The one-side grafted material with a graft yield 5.1 % was selected for mechanical testing because of the "bare hand" feeling of stiffness and the abrasion data in **Figure 29**. **Table 11** lists the tensile properties of grafted and ungrafted materials; the results are the mean values for three samples.

Materials	Modulus (MPa)	Tensile Strength (MPa)	Elongation at Break (%)
Ungrafted polyurethane	$16.8 \pm 0.2$	$37.5 \pm 0.3$	$1060 \pm 43$
5.1 % one-side grafted polyurethane	$17.9 \pm 0.2$	$43.0 \pm 0.4$	$983 \pm 38$

**Table 11.** Tensile properties of grafted and ungrafted polyurethane.

The tensile properties demonstrate that the one-side grafted material is satisfactory and, in some respects, even better than the ungrafted material (tensile strength). Most important of all, **Figure 29** and **Table 11** show that the 5.1 % one-side grafted polyurethane has an improvement in abrasion resistance of a factor of two up to 160 cycles with only a small but acceptable increase (6.5 %) in modulus.

#### 4.5.5.5 Effect of Dose Rate

Double-face grafting by total dose of 10 kGy achieved by 50 Gy/min in 10 % AN/n-hexane solution with 10 min pre-irradiation swelling time was used to investigate the effect of dose rate. The graft yield, 11.7 %, which was slightly larger

than the grafted material synthesized from 210 Gy/min. **Figure 30 and 31** show the smaller dose rate caused smaller graft density on the surface of PAN-g-PU.

#### **4.5.5.5 Permeation and Chemical Resistance**

Dr. Jay Humphrey of the University of Maryland at Baltimore County is at this writing, measuring the permeation properties of our modified polyurethanes. Ms. Dawn Crawford of the Belvoir Research Development and Engineering Center is measuring the resistance of the polyacrylonitrile-modified surface to chemical agents.

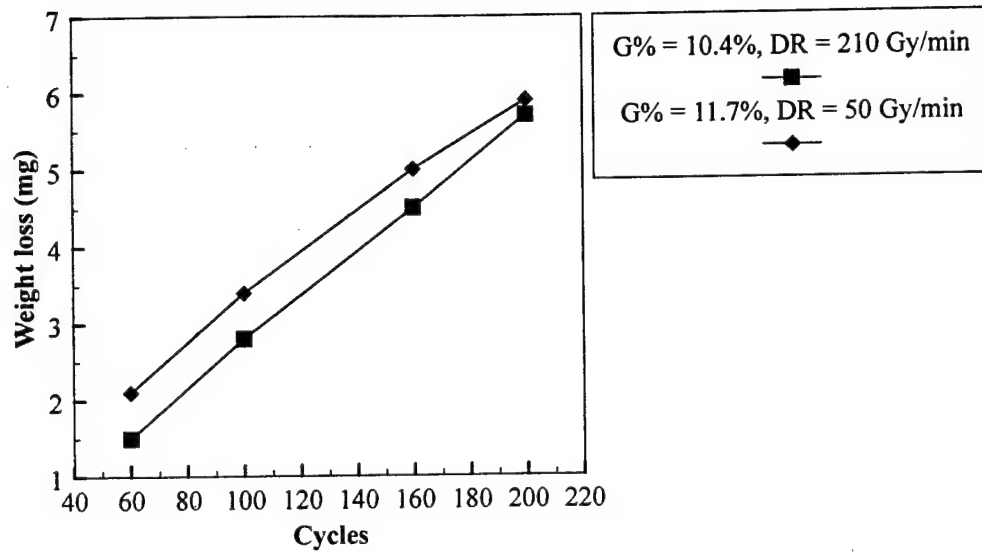


**Figure 30.** Abrasion loss of PAN-g-PU synthesized from different dose rates.

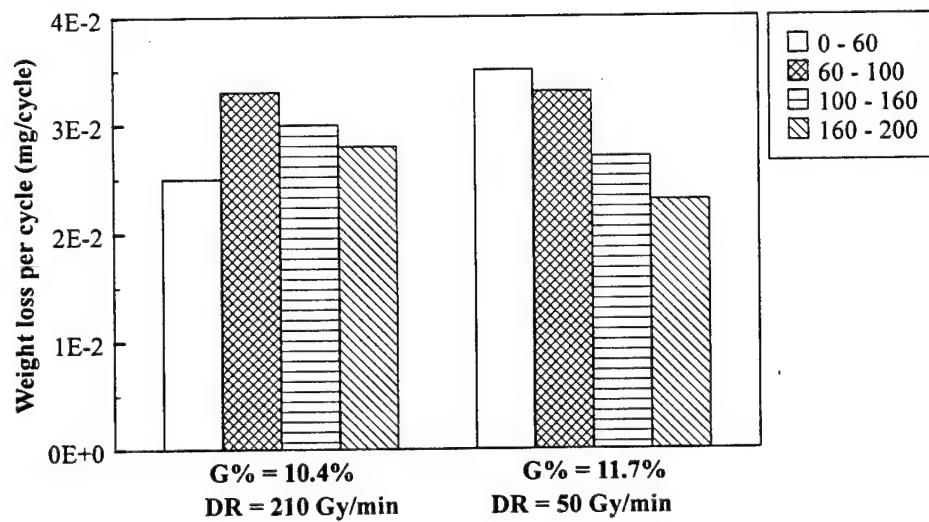


**Figure 31.** Abrasion loss rate of PAN-g-PU synthesized from different dose rates.

## CHAPTER 5

### CONCLUSIONS AND ACCOMPLISHMENTS

1. Twofold improvement in edge abrasion resistance with minimal changes in bulk mechanical properties was achieved by one-sided grafting of polyacrylonitrile to the surface of polyurethane in 10 % AN/n-hexane solution irradiated by a 10 kGy gamma dose.
2. The abrader made by modifying an oscillatory cylinder abrasive machine was successful in measuring the difference in abrasion loss between treated and untreated elastomers.
3. In the curing of acrylated urethane oligomers by cobalt-60 gamma, gel fraction and hardness increase with an increase in absorbed dose. The abrasion resistance is better with larger gel fraction and hardness, which indicates higher crosslinking density results in better abrasion resistance. However, no improvement is found over the conventional polyurethane composite provided by Ft. Belvoir.
4. Low energy electron beam and plasma treatments failed to improve abrasion resistance.
5. A literature study of the theory of abrasion resistance of elastomers was performed and summarized in this work.

## REFERENCES

- [1] R. W. Oertel and R. P. Brentin,, Journal of Coated Fabrics, 22, (1992)
- [2] J. Silverman, Journal of Chemical Education, 58, 168 (1981).
- [3] T. A. Speckhard, K. S. Hwang, S. B. Lin, S. Y. Tsay, M. Koshiba, Y.S. Ding and S. L. Cooper, J. Appl. Polym. Sci., 30, 647 (1985)
- [4]P. Santhana, G. Krishnan,V. Choudhary, and I. K.Varma, J.M.S., Rev. Macromol Chem. Phys., C33(2), 147 (1993)
- [5] H. Kita and Y. Hoshi , Jpn. Kokai Toyoko Koho 61,198,104 (1986); CA, 106, 142198y (1979).
- [6] M. Yoshihara and K. Morikawa, Jpn. Kokai Toyoko Koho 61,111,944 (1986); CA, 105, 213213v (1986).
- [7] V. W. H. Ting, U.S. Patent 4,072,770 (1978).
- [8] C. Decker and K. Moussa, Makromol. Chem., 191, 963 (1990).
- [9] Y. Furumiya and K. Hirai, Jpn. Kokai Toyoko Koho 62,54,711 (1987); CA, 107, 178214p (1987).
- [10] Nippon Synthetic Chemical Industry Co., Jpn. Kokai Toyoko Koho 58,136,672 (1983); CA, 100, 140451f (1984).
- [11] A. Mizuno and A. Takao, Jpn. Kokai Tokkyo Koho 62,285,959 (1987); CA 108, 188589z (1988).
- [12] R. B. Wallace, U.S. Patent 4,325,985 (1982).
- [13] L. P. Harasta, G. M. Leszyk, and E. D. Morrison, U.S. Patent 4,477,548 (1984).

- [14] C. J. Schmidle, *Journal of Coated Fabrics*, 8, 10 (1978).
- [15] T. Ohta, H. Kanbara, A. Dobashi, and Y. Seki, *Radiation Physics and Chemistry*, 25, 465 (1985).
- [16] M. Ando and T. Uryu, *Polymer Journal*, 19, 367 (1987).
- [17] R. W. Seymour and S. L. Cooper, *Macromolecules*, 6, 48 (1973).
- [18] D. C. Allport and A. A. Mohajer, in *Block Copolymers*, D. C. Allport and W. H. Janes, Eds., Applied Science, London, 1973.
- [19] S. L. Cooper and J. C. West, *Encyclopedia of Polymer Science and Technology*, Supplement, No. 1, Wiley, New York, 1978.
- [20] R. Redman, in *Developments in Polyurethanes*, J. M. Buist, Ed., Applied Science Publishers, London, 1978, Chap. 3.
- [21] A. Noshay and J. McGrath, *Block Copolymers - An Overview and Critical Survey*, Academic Press, New York, 1978.
- [22] L. H. Wadhwa and W. K. Walsh, *American Chemical Society, Organic Coating Preparation*, 42, 509 (1980)
- [23] L. H. Wadhwa and W. K. Walsh, *Journal of Applied Polymer Science*, 27, 591 (1982).
- [24] V. V. Shilov, Y. S. Lipatov, L. V. Karabanova, and L. M. Sergeeva, *Journal of Polymer Science, Polymer Chemistry Ed.*, 17, 3083 (1979).
- [25] S. B. Lin, S. Y. Tsay, T. A. Speckhard, K. K. S. Hwang, J. J. Jezerc, and S. L. Cooper, *Chemical Engineering Communication*, 30, 251 (1984).



- [26] G. Spathis, M. Niaounakis, E. Kontou, L. Apekis, P. Pissis, and C. Christodoulides, *Journal of Applied Polymer Science*, 54, 831 (1994).
- [27] J. L. Hong, C. P. Lillya, and C. W. Chien, *Polymer*, 33, 4347 (1992).
- [28] M. Ando and T. Uryu, *Journal of Applied Polymer Science*, 33, 1793 (1987).
- [29] Y. C. Lai and L. J. Baccei, *Journal of Applied Polymer Science*, 42, 2039 (1991).
- [30] W. Oraby and W. K. Walsh, *Journal of Applied Polymer Science*, 23, 3227 (1979).
- [31] W. Oraby and W. K. Walsh, *Journal of Applied Polymer Science*, 23, 3234 (1979).
- [32] M. Koshiha, K. K. S. Hwang, S. K. Foley, D. J. Yarusso, and S. L. Cooper, *Journal of Material Science*, 17, 1447 (1982).
- [33] E. Joseph and G. Wilkes, *Journal of Applied Polymer Science*, 26, 3355 (1981).
- [34] K. Kawate and T. Sasaki, *Polymer Bulletin*, 27, 231 (1991).
- [35] N. Levy and P. E. Massey, *Polymer Engineering Science*, 21, 406 (1981).
- [36] C. Li, R. M. Nagarajan, C. C. Chiang and S. L. Cooper, *Polymer Engineering Science*, 26, 1442 (1986).
- [37] M. Ando and T. Uryu, *Journal of Applied Polymer Science*, 35, 397 (1988).
- [38] M. Ando and T. Uryu, *Polymer*, 29, 370 (1988).
- [39] K. M. Idriss Ali, M. A. Khan, M. M. Zaman, and Hossain, *Journal of Applied Polymer Science*, 54, 309 (1994).
- [40] Z. Wirpsza, in *Polyurethanes: Chemistry, Technology and Applications*, Ellis Horwood Press, New York, chap. 4 (1993).

- [41] T. Tanaka, T. Yokoyama, and Y. Yamaguchi, *Journal of Polymer Science, A-1*, 6, 2153 (1969).
- [42] R. W. Semour, G. H. Estes, and S. L. Cooper, *Macromolecules*, 23, 4351 (1990).
- [43] T. Yokoyama, in *Advances in Urethane Science and Technology*, Vol. 6, 1029, Westport, Technomic (1978).
- [44] S. C. Yoon, Y. K. Sung, and B. D. Ratner, *Macromolecules*, 23, 4351 (1990).
- [45] A. Ballistreri, S. Foti, P. Maravigna, G. Montaudo, and E. Scamporrino, *Journal of Polymer Science: Polymer Chemistry Ed.*, 18 (1923).
- [46] J. H. Saunders and J. K. Backus, *Rubber Chemistry and Technology*, 39, 461 (1966).
- [47] H. H. G. Jellinek and S. R. Dunkle, *Journal of Polymer Science, Polymer Chemistry Ed.*, 21, 487 (1983).
- [48] H. Schultz, *Makromolecule Chemistry*, 172, 57 (1973).
- [49] G. Tarakanov, L. V. Nevskii and V. K. Belyakov, *Journal of Polymer Science, Part C*, 193, 23 (1968).
- [50] E. Dyer and D. W. Osborne, *Journal of Polymer Science*, 47, 2138 (1959).
- [51] H. Okuto, *Makromolecule Chemistry*, 132, 305 (1970).
- [52] C. E. Hoyle, C. P. Chawla, and K. J. Kim, *Journal of Polymer Science, Polymer Chemistry Ed.*, 26, 1295 (1988).
- [53] J. K. Lancaster, in *Polymer Science*, A.D. Jenkins Ed., North Holland, Amsterdam (1972).
- [54] A. Selwood, *Wear*, 4, 311 (1961)

- [55] W. A. Glaeser, *Wear*, 6, 93 (1963)
- [56] O.D.E.C.: Friction, Wear and Lubrication - terms and definitions, Res. Group on  
Wear of Engineering Materials, Paris.
- [57] T. L. Oberle, *Journal of Metals*, 3, 438 (1951).
- [58] B. J. Briscoe, P. D. Evans and J. K. Lancaster, *Wear of Materials*, American  
Society of Mechanical Engineers, New York, 607 (1987).
- [59] A. H. Muhr and A. D. Roberts, *Wear*, 128, 213 (1992).
- [60] K. Friedrich, in *Friction and Wear of Polymer Composites*, Edited by K.  
Friedrich, Elsevier Amsterdam, p 233 (1986).
- [61] J. K. Lancaster, *Wear*, 141, 159 (1990).
- [62] K. A. Grosch and A. Schallamach, *Trans. Inst. Rubber Ind.*, 41, 80 (1965).
- [63] Y. Uchiyama, *Nippon Gomu Kyokaishi*, 57, 93 (1984).
- [64] A. Schallamach, *Prog. Rubber Technol.*, 46, 107 (1984).
- [65] P. Thavamani and A. K. Bhowmick, *Rubber Chemistry and Technology*, 67, 129.
- [66] P. Thavamani and A.K. Bhowmick, *Journal of Material Science*, 28, 1351 (1993).
- [67] P. Thavamani and A. K. Bhowmick, *Rubber Chemistry and Technology*, 65, 31  
(1992).
- [68] A. N. Gent, in *Science and Technology of Rubber*, F. R. Eirich Ed., Academic  
Press, London, 447 (1978).
- [69] K. Mitsuhashi and H. Kaidou, *Nippon Gomu Kyokaishi*, 68, 497 (1995).
- [70] R. M. Evans and J. Fogel, *Journal of Coating Technology*, 49,50 (1977).
- [71] J. Li, and I. M. Hutchings, *Wear*, 135, 293 (1990).

- [72] H. Hofuku, Nippon Gomu Kyokaishi, 68, 662 (1995).
- [73] J. I. Mardel, A. J. Hill, and K. R. Chynoweth, Materials Forum, 16, 155 (1992).
- [74] J. I. Mardel, K. R. Chynoweth, and A. J. Hill, Materials Forum, 19, 117 (1995).
- [75] Report on Nomenclature in the Field of Macromolecules, Journal of Polymer Science, 8, 257 (1952).
- [76] H. A. J. Battaerd and G. W. Tregear, Graft Copolymers, John Wiley & Sons Pub., (1967).
- [77] H. T. Lokhande, P. V. Varadarajan, and N.D. Nachane, Journal of Applied Polymer Science, 48, 495 (1993).